NRL Report 8070

Estimation of the Natural Roll Frequency of a Ship in a Confused Sea

WILSON G. REID

Electromagnetic Studies Projects
Aerospace Systems Branch

April 4, 1977

NAVAL RESEARCH LABORATORY
Washington, D.C.

This report is an edited version of a dissertation submitted in partial fulfillment of the requirements for the degree of Doctor of Philosophy in the Graduate School of Arts and Sciences, University of Pennsylvania, 1975.

REPORT DOCUMENTATION PAGE

READ INSTRUCTIONS BEFORE COMPLETING FORM

1. REPORT NUMBER: NRL Report 8070	2. GOVT ACCESSION NO.
3. RECIPIENT'S CATALOG NUMBER	
4. TITLE *(and Subtitle)*: ESTIMATION OF THE NATURAL ROLL FREQUENCY OF A SHIP IN A CONFUSED SEA	5. TYPE OF REPORT & PERIOD COVERED: Final report on an NRL Problem
	6. PERFORMING ORG. REPORT NUMBER
7. AUTHOR(s): Wilson G. Reid	8. CONTRACT OR GRANT NUMBER(s)
9. PERFORMING ORGANIZATION NAME AND ADDRESS: Naval Research Laboratory, Washington, D.C. 20375	10. PROGRAM ELEMENT, PROJECT, TASK AREA & WORK UNIT NUMBERS: R02-46
11. CONTROLLING OFFICE NAME AND ADDRESS: Naval Electronics System Command, Navy Space Project Office, PME-106, Washington, D.C. 20360	12. REPORT DATE: April 4, 1977
	13. NUMBER OF PAGES: 78
14. MONITORING AGENCY NAME & ADDRESS *(if different from Controlling Office)*	15. SECURITY CLASS. *(of this report)*: Unclassified
	15a. DECLASSIFICATION/DOWNGRADING SCHEDULE

16. DISTRIBUTION STATEMENT *(of this Report)*

Approved for public release; distribution unlimited.

17. DISTRIBUTION STATEMENT *(of the abstract entered in Block 20, if different from Report)*

18. SUPPLEMENTARY NOTES

19. KEY WORDS *(Continue on reverse side if necessary and identify by block number)*

Confused sea
Probability distribution
Roll frequency
Ship roll history
Ship stability
Spectral analysis

20. ABSTRACT *(Continue on reverse side if necessary and identify by block number)*

The natural roll frequency of a ship in a confused sea has been estimated from analysis of the roll history. The estimator was defined, the sources of error were identified, and the parameters of the analysis were selected to minimize the variance of the estimator. The probability distribution was derived for the estimator of the natural roll frequency assuming a Pierson-Moskowitz spectral form for the sea. Bias in the estimator resulting from the steepness of the wave-slope spectrum in the vicinity of resonance and from the finite bandwidth and sidelobe

(Continued)

20. Abstract (Continued)

structure of the spectral window was examined. The results of the theoretical analysis were confirmed by cumulative distribution functions computed from three 4-hr records from the roll history of a light cruiser. Correlations are presented of the estimated natural roll frequency with linear dimension and displacement for a variety of American naval vessels.

CONTENTS

CONTENTS (Continued)

SYMBOLS

A	Arbitrary constant
$A(f)$	Cosine transform of white-noise sample
$A_{n,j}$	Expansion coefficient
$A(\psi_0)$	Function of ψ_0
a	Constant
B	Arbitrary constant
$B(f)$	Sine transform of white-noise sample
$B(f)$	Bias of spectral estimate
$B(T)$	Bias of roll-frequency estimate, function of sample length
$B(V)$	Bias of roll-frequency estimate, function of wind speed
b	Constant
C	Magnitude of $\Gamma(\Theta;f)$ at resonance
$C(\varphi;f)$	Roll power-spectral estimator
$C(\Phi;f)$	Roll power-spectral estimator (random variable)
$C_i(\Theta;f)$	ith wave-normal angle power spectral estimator
$C_i(\Phi;f)$	ith roll power spectral estimator
$\overline{C}(Z_k;f_n)$	Smoothed power spectral estimator (white noise)
c	Wave celerity
$c(\varphi;u)$	Roll sample autocovariance function
$c(\Phi;u)$	Roll sample autocovariance function (random variable)
E	Constant
F	Constant
f	Frequency
f_0	Roll resonant frequency; frequency of sinusoid
f_r	Frequency of unresisted roll in still water
f_s	Sample rate
f_φ	Natural roll frequency
$\hat{f}_\varphi$	Natural-roll-frequency estimator
$\overline{\hat{f}}_\varphi$	Sample mean of natural-roll-frequency estimator

$\hat{f}_\varphi(T)$	Natural-roll-frequency estimator function of sample length T
$\hat{f}_\varphi(V)$	Natural-roll-frequency estimator function of wind speed V
G	Center of gravity
$\overline{GM}$	Metacentric height
$\overline{GZ}$	Righting arm
g	Acceleration due to gravity
$H(\omega)$	Transfer function
$h(t)$	Impulse response
I	Moment of inertia
$K(\sigma;\psi - \psi_0)$	Spreading factor
k	Wave number; radius of gyration
ℓ	Linear dimension
M	Righting moment
m	Number of spectra averaged (M in computer plots)
N	Number of data points in a sample
n	Size of input array of discrete Fourier transform
P	Constant
$p_i(\xi_i)$	Probability density function for spectrum estimate
$p_\varphi(\hat{f}_\varphi)$	Probability density function for estimate of natural roll frequency
Q	Constant
S_1	Sample standard deviation (no averaging)
S_m	Sample standard deviation (m spectra averaged)
$\overline{S}_m$	Mean sample standard deviation (m spectra averaged)
S_m^1	Sample standard deviation (m normalized spectra averaged)
S_m^2	Sample standard deviation (m unnormalized spectra averaged)
T	Sample length; length of truncated sinusoid
T_φ	Natural roll period
$U(t)$	Unit step function
u	Lag of autocovariance function
V	Wind speed
v	Ship velocity
v	Ship speed

$w(t)$	Data window
$W(f)$	Spectral window
$Z(f)$	Fourier transform of white noise
$\{Z_k\}$	Sampled white-noise process
Cov[]	Covariance
Var[]	Variance
Var{}	Variance
$E[]$	Expectation
$E\{\}$	Expectation
$\mathcal{F}\{\}$	Fourier transform
$\mathcal{F}^*\{\}$	Complex conjugate Fourier transform
$\|\|$	Modulus
$\square$	Autocorrelation
$\approx$	Approximate equality
rect(t)	Rectangle or gate function
sinc(t)	$(\sin \pi t)/\pi t$
$\overline{\ }$	(bar) mean or average
α	Constant in Pierson-Moskowitz spectrum
β	Constant in Pierson-Moskowitz spectrum
$\Gamma(m)$	Gamma function
$\Gamma(\Phi;\omega)$	Power spectrum of roll process
$\Gamma(\Theta;\omega)$	Power spectrum of wave-normal process
$\Gamma(\eta;\sigma)$	Wave-height frequency spectrum
$\Gamma(\eta;\sigma,\psi)$	Directional wave-height frequency spectrum
μ	Mean of process
$\gamma(\Phi;u)$	Autocovariance function of roll process
Δ	Displacement
Δf	Frequency spacing of spectral estimates
Δt	Time interval between data points
$\delta(f)$	Dirac delta function
ϵ	Fractional error
η	Wave height

θ	Wave-normal angle
θ_m	Wave-normal maximum angle
Θ	Wave-normal angle (random variable)
κ	Coefficient of roll damping
ν	Degrees of freedom of chi-squared variate
ξ_n	Smoothed power spectral estimate at nth harmonic
σ	Radian frequency
σ^2	Variance of white noise
$\sigma_\epsilon(m)$	Standard deviation for fractional error
$\sigma_{\hat{f}_\varphi}(m)$	Standard deviation for roll-frequency estimate
φ	Roll angle
$\overline{\varphi}$	Roll sample mean
Φ	Roll angle (random variable)
Φ_k	Roll angle sampled (random variable)
χ	Angle between ship heading and wave component
ψ	Angle measured counterclockwise from ship beam
ψ_0	Wind direction from ship beam
ω	Radian frequency of encounter
ω_r	Radian frequency of unresisted roll in still water
$\partial\eta/\partial x$	Wave slope normal to roll axis
$\{\Theta(t)\}$	Wave-normal angle process (continuous)
$\{\Phi(t)\}$	Roll-angle process (continuous)
$\{\Phi_k\}$	Roll-angle process (sampled)

ESTIMATION OF THE NATURAL ROLL FREQUENCY OF A SHIP IN A CONFUSED SEA

INTRODUCTION

Background

Motivation for this study derives from use of the natural roll frequency as a measure of ship stability, a matter of concern to masters, ship owners, and insurers of merchant vessels. This use of the natural period of roll was proposed by Norrby [1]. The classic technique for measuring the natural roll period has been to excite the ship in roll by one means or another and to time the decaying oscillations in still water. At times such a test is not feasible, or conditions of loading may be changed while the ship is under way, requiring the stability to be judged at sea. Here the complexity increases because the roll behavior is no longer deterministic, with the ship being driven in roll by a random sea. This point was raised in the discussion of Norrby's paper where it was argued that the rolling period used as a measure of stability should be the natural period of roll of the ship, and not simply the period of encounter* with the sea. In spite of qualitative statements made by a number of workers, and cited by Norrby in his reply, to the effect that a ship normally rolls in her natural period, a ship may be driven at the frequency of a regular wave. Recognition of this led Vossers [2] to suggest that the roll period for judging stability be measured in a relatively confused sea. However, this still is not sufficient because the master of a ship may not always find himself in a confused sea at a time when the stability must be checked. Nor will the general confusion of the sea always suffice because the lack of any predominant swell or direction to the sea cannot ensure that there will be energy in the sea capable of exciting the ship into resonance.

Since the roll period reflects the character of the sea as well as the resonance properties of the ship and since the most definitive description of the sea is in terms of its spectrum, it appears more useful to consider the roll spectrum in lieu of the roll history, the roll spectrum being the product of the power transfer function of the ship in the roll plane and the appropriate spectrum of the sea. The roll behavior of the ship at sea can then be described in terms of a natural roll frequency and the distribution of its estimates with, perhaps, the sea state or local windspeed as a parameter. Until now this has not been done.

Statement of the Problem

The problem, then, is threefold: (a) to define an estimator of the natural roll frequency of a ship in terms of the behavior observable in a confused sea; (b) to develop, using the techniques of spectral analysis, an algorithm for the optimum processing (optimum in the

*Definitions of terms commonly used in naval architecture and oceanography are given in Appendix A.

Manuscript submitted September 17,1976.

sense of minimum variance in the estimates of the natural roll frequency) of a finite length of roll history; and (c) to find the sampling distribution of the roll-frequency estimates thus determined.

Related Research

A number of studies on ship roll motion have been published since the appearance in 1861 of the classic work of Froude [3], who demonstrated so impressively the principle underlying the motion of a ship in waves: momentary equilibrium obtains when the vertical axis of the ship is normal to the wave surface. Kriloff [4] made the identification between the free (natural) and forced oscillations of a ship and indicated that the irregularity of the sea would continually excite free oscillations. During the next 50 years improvements were made in the theory, culminating in the thorough and systematic treatment by Weinblum and St. Denis [5]. A major shortcoming remained, however, in the assumption of regular waves until St. Denis and Pierson [6] added the statistical description of the sea.

The application of spectral analysis to ship roll histories was foreshadowed by the work of Barber [7] and Williams [8], who found spectra for individual roll records. Barber, who was endeavoring to deduce the frequency spectrum of the sea from a frequency analysis of the rolling and pitching of the ship, noted that the speed and direction of travel of the ship had no influence on the main period of the roll. A major contribution was made by Cartwright and Rydill [9], who, using directional frequency spectra measured by a ship-borne wave recorder, obtained excellent agreement between predicted and measured roll spectra. The merit in Cartwright and Rydill's paper, as pointed out by Palmer in the discussion, lay in the authors' having confirmed the applicability for ship roll motion of the principle of linear superposition. A review of the techniques of spectral analysis and a demonstration of their application to seakeeping was made by Marks [10]. Baitis and Wermter [11] subsequently employed these techniques to obtain measurements of the power spectra of ship motions.

Treatment of the natural roll period has been somewhat intuitive. A number of workers (e.g., [2], [8], [9]) have stated that the natural period predominates for rolling. Norrby [1] suggested that the natural roll period be determined as the average of a number of rolling tests where the ship is caused to roll in still water and the time to swing from, say, starboard to port and back to starboard is noted by stopwatch. Histograms for roll periods were obtained by Langmaack [12], Williams [8], and Norrby and Engvall [13]. The period was variously defined as the time interval between alternate zero crossings, twice the time between adjacent maxima and minima, and the time between successive minima. With normal probability curves fitted to the data, standard deviations on the order of 12 to 23% of the mean were obtained by Norrby and Engvall [13] for some 19 rolling tests. The mean roll period at sea was observed to be within 4.5% of its value for still water.

An empirical correlation between natural roll period and ship size is given by Williams [8] for British warships, assuming geometrical similarity of form and weight distribution. A table of roll periods for Japanese merchantmen and warships is given by Tamiya and Motora [14].

Approach

The problem of estimating the natural roll frequency from the spectral analysis of the roll history of a ship driven by a random sea is a special case in the larger area of system identification. Briefly stated, the modeling, or identification, problem is to find a mathematical description (model) of a dynamic system when a set of inputs and a set of outputs are known. The nature of the system may be completely unknown or, as in the case reported here, because of knowledge of the physics governing the behavior of the system, the form of the equations may be known and only the coefficients need be determined.

The classical technique for solving this problem admits of several approaches:

1. The transfer function is plotted directly as the system is excited by a sinusoidal input of variable frequency.

2. The response of the system to a unit impulse, or unit step function, is measured, and the Fourier transform of the response or its derivative is taken to obtain the transfer function.

3. The response of the system to an arbitrary input is measured, and its transform is found and divided by the transform of the excitation to give the transfer function.

4. Sample spectra are computed from the response to white noise and are averaged to obtain the squared modulus of the transfer function.

The first approach was taken in experiments using model tanks under carefully controlled conditions by Baitis and Wermter [11]. The third approach was taken by Cartwright and Rydill [9] aboard a ship at sea where simultaneous measurements were made of the ship's roll and of the spectrum of the sea by a shipborne wave recorder.

Although the problem addressed in this study is eased somewhat by requiring that only one coefficient be determined, the frequency f_φ for resisted roll in still water (assuming the coefficient κ is known), it is rendered more difficult because the excitation is not known. The problem of system identification without knowledge of the input, in even the limited sense treated here, does not appear to have received much attention. The situation is far from hopeless, however, since our limited knowledge of the input may be all that is required to obtain the limited information we are seeking about the system.

One factor that helps considerably is the signal-like character of the roll history, which will be assumed to be a noise-free measurement. (The quantization noise for the 12-bit quantization of the output of the two-speed synchro yields a signal-to-noise ratio of about 45 dB and is therefore assumed to be zero.)

The approach taken here is to assume that additive noise is zero, so that we may write

$$\Gamma(\Phi;\omega) = |H(\omega)|^2\Gamma(\Theta;\omega)$$

where $\Gamma(\Phi;\omega)$ is the spectrum of the roll process, $H(\omega)$ is the transfer function of the vessel in the roll plane, and $\Gamma(\Theta;\omega)$ is the spectrum of the driving force. Here ω is the radian frequency of encounter of the vessel moving through the sea, $\{\Phi(t)\}$ is the roll-angle process, and $\{\Theta(t)\}$ is the wave-normal angle process for those frequency components normal to the roll axis. As will be shown later (see pp. 13 - 18), the spectrum of the driving force is smooth relative to the transfer function, and hence the resonant frequency f_0 will be biased by an amount depending on the slope of the driving force spectrum in the vicinity of resonance. An estimate of the natural roll frequency f_φ is then obtained from a deterministic relation involving the estimated resonant frequency and the coefficient of roll damping, which normally would have been obtained previously from rolling tests in still water.

The problem of estimating these spectra from finite lengths of the roll history is addressed in the section entitled "Spectral Analysis of Ship Roll History" (pp. 18 - 35). Briefly, we take finite lengths of the roll history, apply a Fourier transform to obtain a finite set of sample spectra, and then average across the set since the expectation of the sample spectrum converges in the limit to the process spectrum as the sample length tends to infinity. Hence we measure

$$\frac{1}{m}\sum_{i=1}^{m} C_i(\Phi;\omega) \approx |H(\omega)|^2 \frac{1}{m}\sum_{i=1}^{m} C_i(\Theta;\omega)$$

where $C_i(\Phi;\omega)$ is the ith sample roll spectrum and $C_i(\Theta;\omega)$ is the ith sample spectrum of the driving force. The notation is that of Stilwell and Pilon [15] and distinguishes between the first parameter in the argument as the variable being transformed and the second parameter, which is the independent variable, the frequency.

Since the roll history is a stochastic process, the sample roll spectrum is a random variable and so, therefore, is the roll-frequency estimator $\hat{f}_\varphi$. The questions that remain to be answered then are the following:

1. Given a finite length of roll history, what is the algorithm for the optimum (minimum variance) processing of the data?

2. What is the sampling distribution for the roll-frequency estimates?

3. What is the bias in the roll-frequency estimates due to the steepness in the spectrum of the driving-force in the vicinity of resonance and that due to the finiteness of the sample lengths processed?

To answer the first question a parametric analysis is conducted in which the following parameters are varied: the sample length T, the number m of spectra to be averaged, the shape of the data window $w(t)$, and the method of averaging. From this it is determined that the optimum selection of parameters is to make the sample length T equal to the decorrelation time of the roll record, to make the number m of spectra to be averaged as

large as possible, to use a rectangular data window $w(t)$, and to average normalized power spectra computed from noncontiguous portions of the roll record.

To answer the second question, we model the ship by a linear system with an input of white noise. For resisted rolling in still water, the transfer function of the linear system is that of the ship in the roll plane. For resisted rolling among waves, the transfer function of the linear system is the product of the transfer function of the ship in the roll plane and the square root of the spectrum of the driving force, based on a theoretical model of the sea due to Pierson and Moskowitz [16]. A transformation is made from the probability distribution of the spectral estimates for the simulated roll spectrum to the probability distribution of the estimates of the natural roll frequency. Complementing the theoretical study are measurements of the natural roll frequency made from 12 hr of roll data from the USS *Providence*. Both the model and the measurements indicate that the estimates of the natural roll frequency are normally distributed.

To answer the third question, we assume that the variance in the spectral estimates is zero, implying, in principle, that an infinite number of sample spectra are available for averaging. For the case of simulated still-water rolling, bias arises from convolution of the spectrum of the roll process with a spectral window of width inversely proportional to the sample length. For simulated rolling among waves, bias arises from the aforementioned convolution and from the steepness in the spectrum of the driving force in the vicinity of resonance. For both types of rolling, the bias in the roll-frequency estimator is tabulated as a function of sample length. We isolate the bias due to the steepness in the spectrum of the driving force in the vicinity of resonance by making both assumptions: zero variance and infinite sample length. In this case bias in the estimator of the natural roll frequency is tabulated as a function of wind velocity, which, for a fully developed sea, determines the shape of the spectrum of the driving force. These points are covered in detail on pp. (30 - 39).

Contributions

Several contributions are made in this study to the problem of ship roll behavior. These include the following:

1. An operative definition of the estimator of the natural roll frequency in terms of the observable behavior of a ship in a confused sea

2. Identification of the sources of error in estimating the natural roll frequency from such behavior

3. Formulation of an algorithm for the optimum processing of a finite length of roll history (optimum in terms of minimum variance in the estimate of the natural roll frequency)

4. A derivation of the probability distribution for the estimates of the natural roll frequency

5. An assessment of the bias in the estimate of the natural roll frequency due both to finite sample lengths and to the steepness in the spectrum of the driving force in the vicinity of resonance

6. Recognition that large-amplitude rolling derives not so much from proximity to resonance, as has been supposed, but from some other cause (e.g., coherence of the wave train driving the ship in roll)

7. A correlation between ship-size parameters and the natural roll frequency for a variety of American naval vessels.

It was pointed out in the review of related research how a more intuitive definition of the roll period (applied to an aperiodic function) led to distributions with large variances. The definition of the natural roll frequency is made more precise by assuming the roll spectrum to be the product of the transfer function in the roll plane and the appropriate spectrum of the sea that drives the ship in the roll plane as a linear, uncoupled oscillator. This assumption has been shown to be valid over an important range of values of roll angle and ship speed. The natural roll frequency, or the frequency of resisted roll in still water, is defined in terms of the roll-damping coefficient and the resonant frequency, or peak of the transfer function. The errors in estimating the natural roll frequency from measurements of the frequency of the peak in the roll spectrum are attributable to (a) errors in the determination of the roll-damping coefficient, (b) bias in the frequency of the resonant peak because of the steepness in the spectrum of the driving force in the vicinity of resonance, and (c) the variance and bias in the spectral estimates resulting from processing finite lengths of the roll history.

A parametric analysis showed that large-amplitude rolling, contrary to the opinion expressed by Vossers [2] and Williams [8], derives not so much from proximity to resonance as from other causes (possibly coeherence of the wave train in the sea). This was discovered by a comparison of averaging techniques. It was argued that if large-amplitude rolling were the result of proximity to resonance, then the heavier weighting given to spectra from such portions of the record by averaging unnormalized power spectra would give a smaller variance in the measurement than would be given by normalized power spectra. It was found that this was not the case; averaging normalized power spectra (thereby giving each portion of the record equal weight regardless of the amplitude of the oscillations) led to the smaller variance.

An optimum processing scheme based on the decorrelation time of the roll history being examined was deduced. Given a roll record of arbitrary length, the minimum variance in the measurement of the natural roll frequency is achieved by (a) subdividing the record into m segments T seconds long, where T is the decorrelation time of the record (the lag at the first minimum of the envelope of the autocorrelation function); (b) adding zeros to achieve the desired fineness in frequency (an interpolation method); (c) transforming to obtain the power spectra; (d) normalizing the power spectra to unity total power; (e) averaging the normalized power spectra; and (f) locating the global maximum in the magnitude of the resulting spectrum. The variance can be further reduced if, instead of subdividing a continuous record into m segments, the m segments are taken from noncontiguous portions of the roll history over a longer period of time.

Included in the study is a comparison of the natural-roll-frequency cumulative distribution functions for several values of the processing parameters for the USS *Providence* and a correlation with ship-size parameters of the measured natural roll frequencies for a variety of American naval vessels.

Of theoretical interest is an investigation of the variance and bias in the estimate of the resonant frequency of a linear system when the input is white noise. The variance arises as a result of averaging the spectra from a finite number of realizations from the ensemble of possible realizations of the process, whereas the bias is induced by transforming a finite length of each of the infinite number of realizations to obtain the spectra to be averaged. These two effects are studied separately: the variance by assuming a finite number of realizations of infinite length (zero-bias case) and the bias by assuming an infinite number of realizations of finite length (zero-variance case).

The effect of these considerations on the estimator of the natural roll frequency is assessed by assuming two linear systems in tandem fed by white noise and having transfer functions equivalent to (a) the square root of the Pierson-Moskowitz [16] wave-slope spectrum that drives the ship in roll and (b) the transfer function of the ship in the roll plane. In the absence of bias, the estimator of the natural roll frequency was found to be normally distributed, a condition deriving from the high degree of symmetry in the overall transfer function in the vicinity of resonance and the very rapid decrease in the probability away from resonance. The bias, which is due to leakage of power through the sidelobes of the spectral window in the convolution between the spectral window and the spectrum of the process (in this case the overall transfer function), accounts for a downward shift in the estimate of the resonant frequency because of the particular asymmetry in the transfer function (higher below resonance and lower above resonance).

To demonstrate the effects of bias from leakage for the case of short sample lengths (a few cycles of the process) an analysis of the error in estimating the frequency of a truncated sinusoid is included as Appendix A. This analysis emphasizes the effect of leakage from the negative-frequency image, which can be substantial when the record to be transformed is short and the spectrum has a few dominant "lines."

Synopsis

The section that follows, "Roll Behavior of a Ship at Sea," discusses the roll behavior of a ship at sea and the major assumptions required in this study. The equation of motion in the roll plane (linear and uncoupled) and its solution are given. From this the natural roll frequency, or frequency of resisted rolling in still water, is identified. Also identified from the solution of the equation of motion is the transfer function. From this is found the roll resonant frequency (the peak of the transfer function). A deterministic relation is then found for the natural roll frequency in terms of the roll resonant frequency and the coefficient of roll damping. The coefficient of roll damping, its effect on the linearity assumption, and a method for its measurement are next discussed. Finally, the spectrum of the driving force is defined and expressed in terms of the one-dimensional frequency spectrum for the wave heights. This spectrum is the most easily measured and has been modeled for fully developed seas by several workers, most recently by Pierson and Moskowitz

[16]. Several examples of the spectrum of the driving force are given; when compared with the squared modulus of the transfer function, they give some idea of the effect of the former on the roll spectrum and on the estimate of the natural roll frequency.

The next section, "Spectral Analysis of Ship Roll History," treats the aspects of the theory of spectral analysis that are necessary to an appreciation of the problems in deriving the probability distribution for the estimates of the natural roll frequency. First a 2-hr sample from the roll history of the USS *Providence* is reproduced and some basic assumptions are discussed. Then the power spectrum of the roll process is defined as the Fourier transform of the autocovariance function of the roll stochastic process. Next discussed is a method for estimating the roll spectrum when finite lengths of the roll history are available for processing. The distributional properties of power-spectral estimators are reviewed, and this information is used to derive the probability distribution for the estimator of the natural roll frequency. The section concludes with a discussion of the bias in the estimator of the natural roll frequency resulting from processing finite-length samples of the roll history and from the steepness in the spectrum of the driving force in the vicinity of resonance.

The spectral analysis method is then applied to actual roll histories from a variety of American naval vessels. This section of the report begins with a summary of the conditions under which the data were gathered and then discusses considerations in the selection of the parameters for the processing of the data. It then reports the results of processing 12 hr of roll history from the USS *Providence* and shows that with appropriate processing the spectral analysis of ship roll history may yield an estimate of the natural roll frequency with very small variance. This discussion concludes with correlations of the natural-roll-frequency estimates for a variety of American naval vessels with various size parameters (length, beam, draft, and displacement). These correlations are presented with a view to using measurements of the natural roll frequency, if such measurements could be extracted from radar data, as a means of classifying radar targets.

Appendix A, on the error in estimating the frequency of a truncated sinusoid by spectral analysis, is included to help explain the source of some of the variability in the estimates of the natural roll frequency based on short sample lengths.

ROLL BEHAVIOR OF A SHIP AT SEA

Equation of Motion

The equation of motion in the roll plane for a vessel experiencing resisted rolling in regular, beam seas† is given [17], with a slight change in notation, as

$$\frac{d^2\varphi}{dt^2} + 2\omega_r \kappa \frac{d\varphi}{dt} + \omega_r^2 \varphi = \omega_r^2 \theta_m \sin \omega t \qquad (1)$$

† Definitions of terms commonly used in naval architecture and oceanography are given in Appendix B.

where

ω_r = the radian frequency for unresisted rolling in still water

ω = the radian frequency of the waves driving the ship in roll

θ_m = the angle of the maximum wave slope

κ = the coefficient of roll damping (differing from that given in the cited work by a factor of π^{-1})

φ = the roll angle

The general solution to this linear, second-order differential equation with constant coefficients, which can be verified by substitution, is given by

$$\varphi(t) = \left[\left(1 - \frac{f^2}{f_r^2}\right)^2 + 4\kappa^2\left(\frac{f}{f_r}\right)^2\right]^{-1/2} \times \theta_m \sin\left\{2\pi ft - \tan^{-1}\left[2\kappa\left(\frac{f/f_r}{1 - f^2/f_r^2}\right)\right]\right\} + ae^{-2\pi\kappa frt} \sin\left[2\pi f_r(1 - \kappa^2)^{1/2}t + b\right] \quad (2)$$

where a and b are arbitrary constants to be determined from the initial conditions and where the frequencies f_r and f are equal to $\omega_r/2\pi$ and $\omega/2\pi$.

Natural Roll Frequency

The second term in Eq. (2) is the transient response consisting of a damped oscillation at the natural frequency

$$f_\varphi = f_r(1 - \kappa^2)^{1/2}. \quad (3)$$

It is this frequency, the natural roll frequency for resisted rolling in still water, that is observed in rolling tests in calm water alongside a wharf where a heave with a crane to a bollard or in a harbor where a sharp maneuver of the rudder is sufficient to excite the damped oscillations characterizing the transient response. If we take the time between alternate zero crossings as the period of the oscillation, the average of several such rolling tests should be expected to give a measurement of the natural roll frequency with a reasonably small variance.

Coefficient of Roll Damping

Because of the detrimental effects of rolling — such as structural stress, shipping of water, discomfort to passengers and crew, damage from shifting cargo, and in extreme cases capsizing — the damping of roll motion has received considerable attention. The interested reader is referred to Refs. 2, 5, 6, 17, and 18 for a more extensive treatment

of the topic and for additional references. The intent here is simply to demonstrate what may reasonably be taken as the coefficient of roll damping for the ships under study and to show that in the appropriate regime of ship speed or of roll angle the damping can be assumed to be linear.

Briefly, roll damping is attributable to two phenomena: (a) wave generation, which varies linearly with velocity; and (b) viscous damping, which varies as the square of the velocity and arises from friction and from flow separation over bilge keels. Lalangas [19] showed, from model studies, that damping was linear for roll angles not exceeding about 10 degrees. For the data analyzed on pp. 38 - 54, the USS *Providence* exhibited a maximum roll angle of about 7.5 degrees. It was assumed, therefore, that roll damping was linear.

The value of the coefficient of roll damping is normally determined from rolling tests in still water by comparing the exponent in the transient response, the second term in Eq. (2), with the envelope of the damped oscillations. An alternative approach, described by Cartwright and Rydill [9], is to use the envelope of the autocorrelation function, which, if the spectrum of the driving force is uniform in the vicinity of resonance and if the rolling is linear, is identical with the envelope of the decaying oscillations in still water. The equivalence can by explained by noting that for the assumed conditions the roll spectrum is essentially the square of the modulus of the transfer function scaled in amplitude by a constant equal to the amplitude of the spectrum of the driving force. The autocorrelation function of the roll process, which by the Wiener-Khintchine theorem [20,21] is the Fourier transform of the roll spectrum, is therefore the autocorrelation function of the impulse response. For positive arguments the autocorrelation function of the impulse response is functionally identical with the impulse response, differing only in amplitude and phase. Since the impulse response is simply a member of the set of all possible transient responses, the equivalence follows. Stated mathematically,

$$\Gamma(\Phi;f) = |H(f)|^2\ \Gamma(\Theta;f)$$

$$\approx C|H(f)|^2$$

$$\gamma(\Phi;u) \approx Ch(t) \square h(t)$$

where C is the magnitude of $\Gamma(\Theta;f)$ in the vicinity of resonance, $\gamma(\Phi;u)$ is the autocorrelation function of the roll process, $h(t)$ is the impulse response of the ship in the roll plane (the Fourier transform of the transfer function), $\approx$ denotes approximate equality, and the symbol $\square$ denotes autocorrelation. From the transient term in Eq. (2) we can write the impulse response as

$$h(t) = Ae^{-at} \sin(bt + B)\ U(t)$$

where A and B are the arbitrary constants appropriate to the impulse response, $U(t)$ is the unit step function, and for simplicity $a = 2\pi f_r \kappa$ and $b = 2\pi f_r (1 - \kappa^2)^{1/2}$. With this expression for the impulse response, the autocorrelation function for the roll process may be written, for $u > 0$, as

$$\gamma(\Phi;u) \approx C \int_{-\infty}^{\infty} Ae^{-at} \sin(bt + B)\, U(t) Ae^{-a(t+u)} \sin[b(t+u) + B]\, U(t+u)\, dt$$

$$\approx CA^2 e^{-au} \int_{\max(0,-u)}^{\infty} e^{-2at} \sin(bt + B) \sin[(bt + B) + bu]\, dt$$

$$\approx CA^2 e^{-au} \int_{0}^{\infty} e^{-2at} \sin(bt + B)\, [\sin(bt + B) \cos bu + \cos(bt + B) \sin bu]\, dt$$

$$\approx CA^2 e^{-au} \left[\cos bu \int_{0}^{\infty} e^{-2at} \sin^2(bt + B)\, dt + \sin bu \int_{0}^{\infty} e^{-2at} \sin(bt + B) \cos(bt + B)\, dt \right]$$

$$\approx CA^2 e^{-au}(P \cos bu + Q \sin bu)$$

$$\approx Ee^{-au} \cos(bu - F)$$

where P and Q are equal to the integrals multiplying cos bu and sin bu and where $E = CA^2\ (P^2 + Q^2)^{1/2}$ and $F = \tan^{-1}\ (Q/P)$. This shows the equivalence of the exponent in the autocorrelation function above and the exponent in the transient response.

Assuming for the moment that the above conditions are met, we find from examination of the autocorrelation function estimator in Fig. 1 that the envelope of the decaying oscillations decreases to e^{-1} of its initial value by about 27 sec, which yields a roll-damping coefficient equal to 0.081, assuming a frequency f_r for unresisted roll in still water of 0.0731 Hz. This value differs from the value cited in Ref. 17 as normally obtaining — that is, $\kappa = 0.032$. The difference between these two values is probably attributable to a broadening of the resonant peak in the roll spectrum due to the steepness in the spectrum of the driving force in the vicinity of resonance.

To check the validity of this hypothesis, we computed simulated roll spectra for several windspeeds by taking the product of the power transfer function and spectra of the driving force derived from the Pierson-Moskowitz spectrum [16] (pp. 12 - 18). The half-power bandwidth of the resonant peak in the roll spectrum was identical (to better than 0.0001 Hz) with that of the power transfer function for windspeeds above 20 m/sec. At 10 m/sec there was significant broadening of the resonant peak. At low windspeeds the peak of the transfer function lies to the left of the peak in the spectrum of the driving force where the rate of change of power with frequency is the greatest.

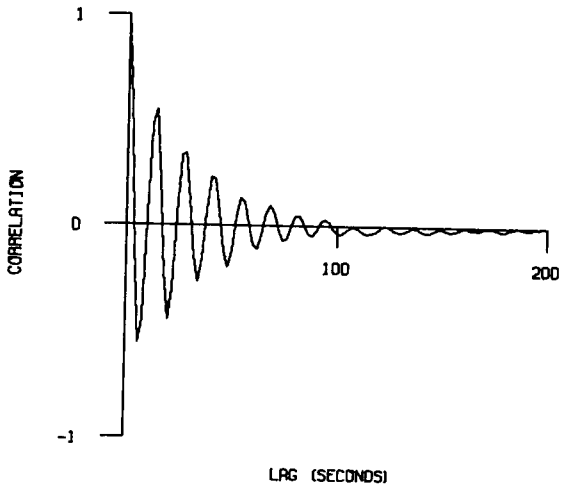

Fig. 1 — Autocorrelation-function estimator for 4 hr of roll data from the USS *Providence* (CLG-6), February 16, 1972

Roll Transfer Function

The transfer function, which gives the amplitude and phase of the response of the vessel to sinusoidal driving functions of arbitrary frequency, can be deduced from the steady-state term of Eq. (2) to be

$$H(f) = \left[\left(1 - \frac{f^2}{f_r^2}\right)^2 + 4\kappa^2 \frac{f^2}{f_r^2}\right]^{-1/2} \exp\left\{i \tan^{-1}\left[2\kappa\left(\frac{f/f}{1 - f^2/f_r^2}\right)\right]\right\}. \quad (4)$$

The square of its modulus is plotted in Fig. 2. The modulus peaks at the roll resonant frequency f_0, which varies, as seen in the figure, with the coefficient of roll damping. For the small values of the coefficient that normally obtain (i.e., for $\kappa \approx 0.032$), the resonant frequency departs little from the natural roll frequency that we are endeavoring to estimate.

The relationship between the roll resonant frequency f_0 and the natural roll frequency f_φ (the frequency of resisted rolling in still water) can be found by maximizing the modulus of Eq. (4). The result is

$$f_0 = f_r (1 - 2\kappa^2)^{1/2}. \quad (5)$$

Substitution of Eq. (5) into Eq. (3) for the frequency of unresisted rolling in still water yields

$$f_\varphi = f_0 \left(\frac{1 - \kappa^2}{1 - 2\kappa^2}\right)^{1/2}. \quad (6)$$

For a nominal coefficient of roll damping of 0.032, the radical above equals 1.0005, so that there is no appreciable difference between the natural roll frequency and the resonant frequency.

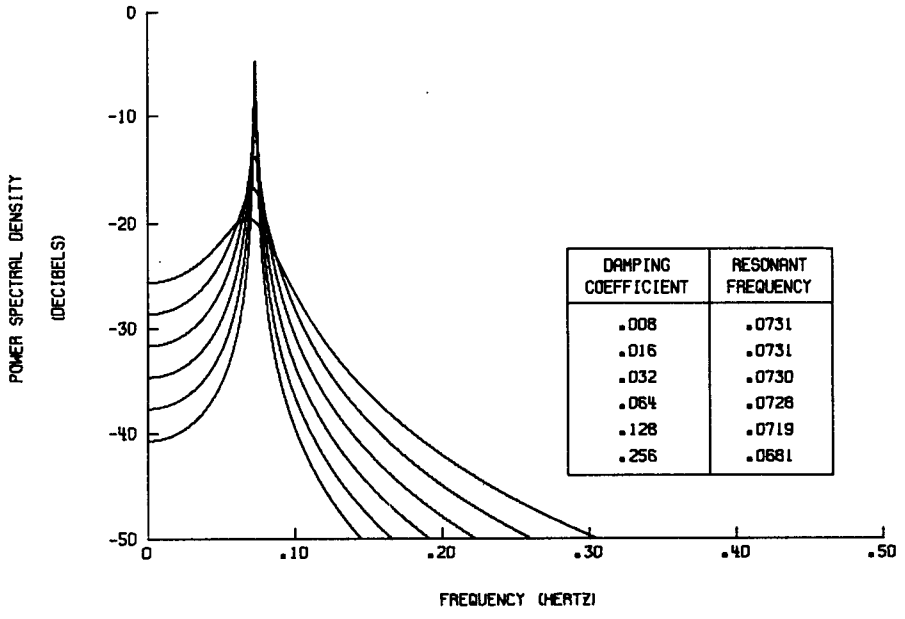

Fig. 2 — Squared modulus of the transfer function in the roll plane vs coefficient of damping

Under such conditions we may properly define the natural roll frequency as the frequency at which the modulus of the transfer function peaks.

Spectrum of the Driving Force

It was previously pointed out that if the spectrum of the driving force is smooth relative to the transfer function, the global maximum in the roll spectrum will approximate the roll resonant frequency f_0 with a bias dependent on the steepness in the spectrum of the driving force in the vicinity of resonance. It is the purpose of this section to give an expression for the spectrum of the driving force and to show that it can be assumed to be smooth.

As shown by Longuet-Higgins et al. [22], the frequency spectrum of the wave slope along the x axis may be written

$$\Gamma\left(\frac{\partial \eta}{\partial x};\sigma\right) = \int_0^{2\pi} k^2 \cos^2 \psi \; \Gamma(\eta;\sigma,\psi) \, d\psi \tag{7}$$

where

η = the wave height

σ = the radian frequency

k = the wave number

ψ = the polar angle measured counterclockwise from the positive x axis

The notation, due to Stilwell [15], shows explicitly that $\Gamma\ [(\partial\eta/\partial x);\sigma]$ is the spectrum of the wave slope $\partial\eta/\partial x$ along the x axis and is a function of the frequency σ. The directional, wave-height, frequency spectrum $\Gamma(\eta;\sigma,\psi)$ gives both the frequency σ and direction of travel ψ of the wave components making up the wave height $\eta(t)$ at a given point in the ocean.

From Eq. (1) the driving force for beam seas is seen to be induced by the angle $\theta(t)$ that the surface of the wave makes with the horizontal or, equivalently, that the wave normal makes with the vertical. For oblique seas the angle $\theta(t)$ can be defined as

$$\theta(t) = \tan^{-1} \frac{\partial \eta}{\partial x} \tag{8}$$

where the x axis is normal to the roll axis and to the local vertical. For small wave slopes the arctangent can be approximated by its argument. Expressions for the mean square slopes presented by Cox and Munk [23,24] indicate that, for wind velocities as high as 50 m/sec, the rms value of the angle $\theta(t)$ for the larger gravity waves is only 16 degrees. Hence we can write for the spectrum of the driving force in Eq. (1) in the case of oblique seas

$$\Gamma(\theta;\sigma) \approx \int_0^{2\pi} k^2 \cos^2 \psi\ \Gamma(\eta;\sigma,\psi)\ d\psi. \tag{9}$$

The directional frequency spectrum $\Gamma(\eta;\sigma,\psi)$ is related to the one-dimensional frequency spectrum $\Gamma(\eta;\sigma)$ for the wave height $\eta(t)$ by the expression

$$\Gamma(\eta;\sigma,\psi) = \frac{1}{\sigma} \Gamma(\eta;\sigma)\ K(\sigma;\psi\text{-}\psi_0) \tag{10}$$

where ψ_0 is the wind direction and where the spreading function $K(\sigma;\psi\text{-}\psi_0)$ may, in general, be a function of the frequency σ. Kitaigorodskii [25] lists several spreading functions, among which

$$K(\sigma;\psi\text{-}\psi_0) = \begin{cases} \dfrac{8}{3\pi} \cos^4 (\psi\text{-}\psi_0), & |\psi\text{-}\psi_0| < \dfrac{\pi}{2} \\ 0 \quad \text{otherwise} \end{cases} \tag{11}$$

seams particularly simple but adequate for our purposes. Substituting Eqs. (10) and (11) into Eq. (9) gives

$$\Gamma(\theta;\sigma) \approx \frac{k^2}{\sigma} \Gamma(\eta;\sigma) \int_{\psi_0-\pi/2}^{\psi_0+\pi/2} \frac{8}{3\pi} \cos^2 \psi\ \cos^4 (\psi\text{-}\psi_0)\ d\psi$$

$$\approx \frac{\sigma^3}{g^2} \Gamma(\eta;\sigma)\ A(\psi_0) \tag{12}$$

where $A(\psi_0)$ is equal to the integral in the line above. Use has been made of the dispersion relation $\sigma^2 = gk$ for waves in deep water, g being the acceleration due to gravity.

Because of the impact of adverse sea conditions on shipping, there have been efforts (see, for example, Refs. 16, 26, and 27) to characterize the sea by means of enery spectra with wind velocity as a parameter. The spectral form given by Pierson and Moskowitz [16] for a fully developed sea is

$$\Gamma(\eta;\sigma) = \frac{\alpha g^2}{\sigma^5} \exp\left[-\beta\left(\frac{g}{V\sigma}\right)^4\right] \tag{13}$$

where V is the windspeed, σ is the radian frequency, and α and β are dimensionless constants equal to 0.0081 and 0.74, respectively. Use of the Pierson-Moskowitz spectrum in Eq. (12) yields

$$\Gamma(\theta;\sigma) \approx \frac{\alpha}{\sigma^2} \exp\left[-\beta\left(\frac{g}{V\sigma}\right)^4\right] A(\psi_0) \tag{14}$$

where $A(\psi_0)$ is a function only of wind direction ψ_0. This will be referred to as a Pierson-Moskowitz wave-slope spectrum, shown in Fig. 3 for several windspeeds. The point to be noted is the smoothness of the spectrum and the slope over the band of frequencies from 0.04 to 0.12 Hz within which the natural roll frequency of most ships would be expected to fall.

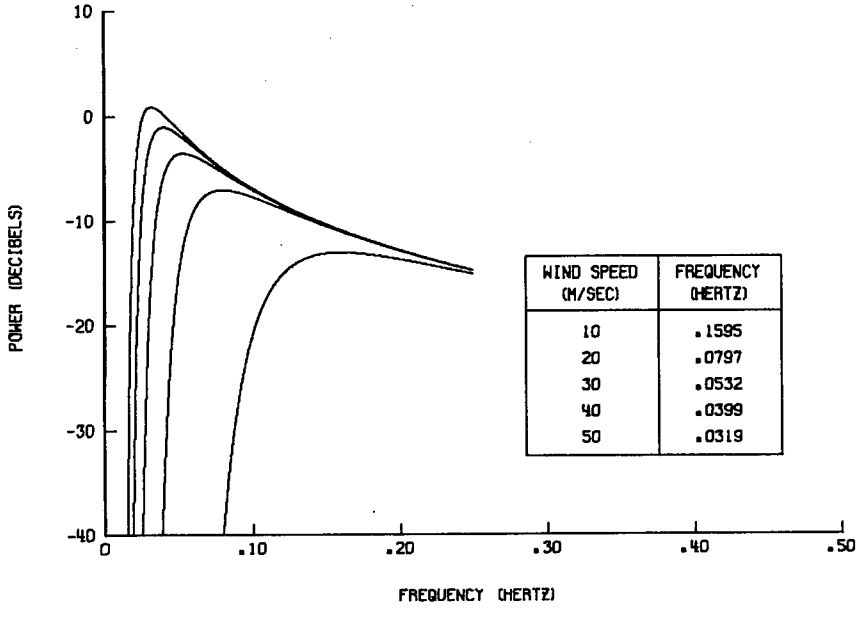

Fig. 3 — Wave-slope spectra vs wind speed from Pierson-Moskowitz spectrum

Since the Pierson-Moskowitz spectrum represents the average of a great many spectra, one might properly ask what a short-term spectrum, based on the amount of ship-roll data that would likely be available for processing would look like. Figures 4 through 6 show the wave-slope frequency spectrum for wave-height data from Argus Island, a platform off the coast of Bermuda. Figure 4 is a typical spectrum corresponding to 100 sec of data, whereas Fig. 5 is an average of 12 such spectra with rectangular weighting. Figure 6 is an average of the same 12 spectra, but the data has been weighted by a data window corresponding to $\sin^4(\pi t/T)$, where T is the sample length. The reason for weighting the data is to achieve a spectral window with desirable characteristics. This point is discussed further on pp. (28 - 30).

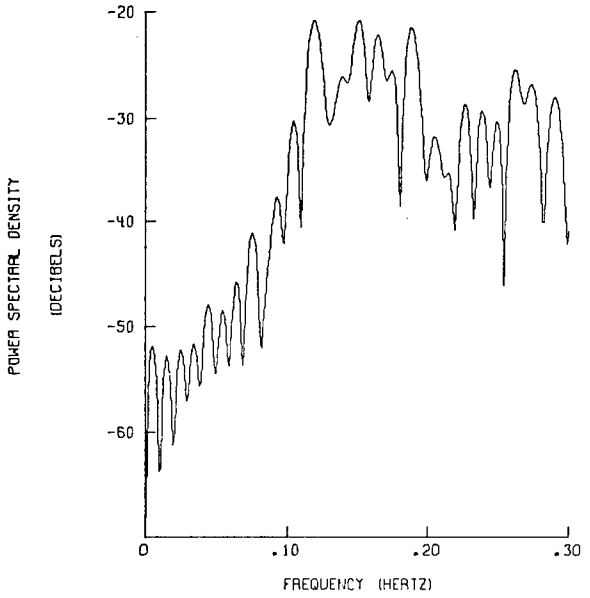

Fig. 4 — Slope spectrum of wave-height record from Argus Island for 100 sec of data

An obvious feature of the spectrum of Fig. 4 is its noiselike character over the band of frequencies from 0.04 to 0.12 Hz. This variability decreases with averaging, as shown in Fig. 5. By choosing a spectral window with lower sidelobes than those of the sinc-function spectral window employed in Figs. 4 and 5, the spectrum is made smoother over the range of interest.

Equation (14) for the spectrum of the driving force is deficient in one detail since for a ship moving with a velocity v through the sea the frequency components in the sea are doppler-shifted by an amount $\sigma(v/c)\cos\chi$ to give a frequency of encounter

$$\omega = \sigma\left(1 - \frac{\sigma v}{g}\cos\chi\right) \tag{15}$$

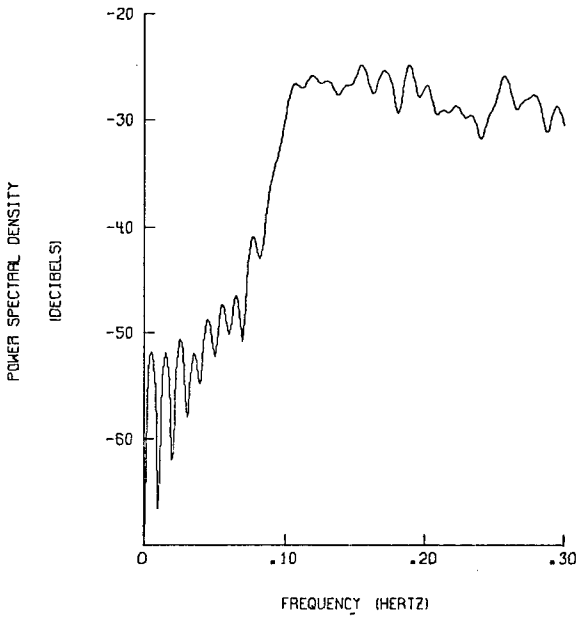

Fig. 5 — Slope spectrum of wave-height record from Argus Island resulting from averaging twelve 100-sec spectra with rectangular weighting

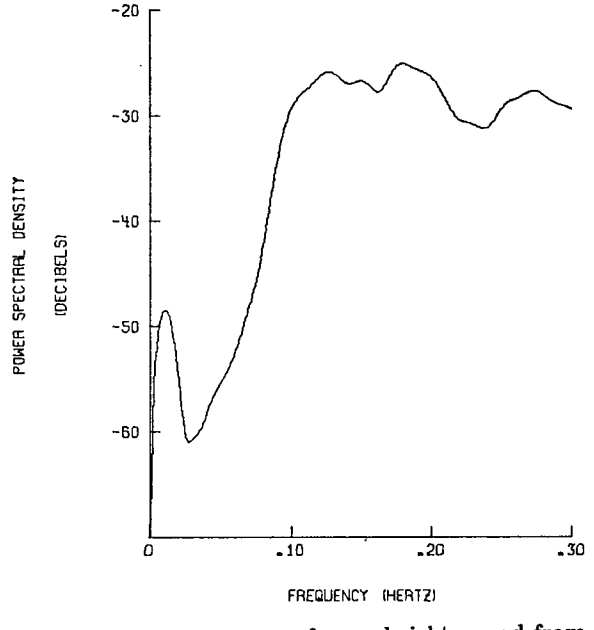

Fig. 6 — Slope spectrum of wave-height-record from Argus Island resulting from averaging twelve 100-sec spectra with $\sin^4(\pi t/T)$ weighting

where $c = g/\sigma$ is the wave celerity, v is the ship speed, and χ is the angle between the ship heading and the wave direction. The inverse transformation from ω to σ is not unique, and the mathematics of the transformation to an encounter spectrum become quite tedious. The reader interested in the details of the transformation is referred to Refs. 6 and 28.

Intuitively, we would expect that frequency components in the sea within a small angle of the bow or stern of the ship would be shifted in frequency by rather large amounts, whereas components coming from abeam would barely be shifted. Since it is the frequency components from abeam that are most effective in exciting the ship in roll, it would appear that the encounter spectrum for the driving force would not differ appreciably from that given by Eq. (14).

Moreover, the low-frequency waves in the vicinity of resonance have a higher celerity and are therefore shifted proportionately less in frequency. Also, for the ship motion histories discussed in this report, the speed of the ship was rather low, being only 6 knots, so that for these cases the doppler shift would be small. For a resonant frequency of 0.0730 Hz, the maximum doppler shift would be only 0.0015 Hz for waves at the frequency of roll resonance coming from ahead or astern.

SPECTRAL ANALYSIS OF SHIP ROLL HISTORY

Roll Stochastic Process

Ship roll histories (e.g., Fig. 7) are time series — that is, random, or nondeterministic, functions of time due to the randomness of the sea that drives the ship in roll. These histories are characterized by the fact that future behavior cannot be predicted exactly from knowledge of the past. Two records from the same time series, though differing in detail, may nevertheless show similarities in their statistical, or average, properties. Hence one pictures a particular roll history as one realization of a stochastic process described by a set of random variables $\{\Phi(t)\}$ and the joint probability distribution associated with each of the times t. Although the time series represented by the ship's roll history is continuous, the need to process data on a digital computer will require that they be sampled at discrete times.

Some important assumptions are normally made in time-series analysis for the sake of tractability of the mathematics. One of these assumptions is stationarity, which implies that the process is in statistical equilibrium. Lack of stationarity, or nonstationarity, implies that the statistical properties change with time. For example, the violence of the motion of a ship at sea increases with the sea state, or in the case of roll the amplitude of the oscillations is greatest when the ship is on a heading that places it broadside to the predominant direction of the sea. In these cases the variance of the roll angle is a function of time as the ship alters course or as the weather changes, thereby affecting the sea state. The roll history may also exhibit bias due to heeling of the ship under the influence of a strong wind that is itself random. Hence the roll hsitory is stationary over limited times only. Since these times are normally much longer than the duration of the records being processed, the assumption of stationarity is made.

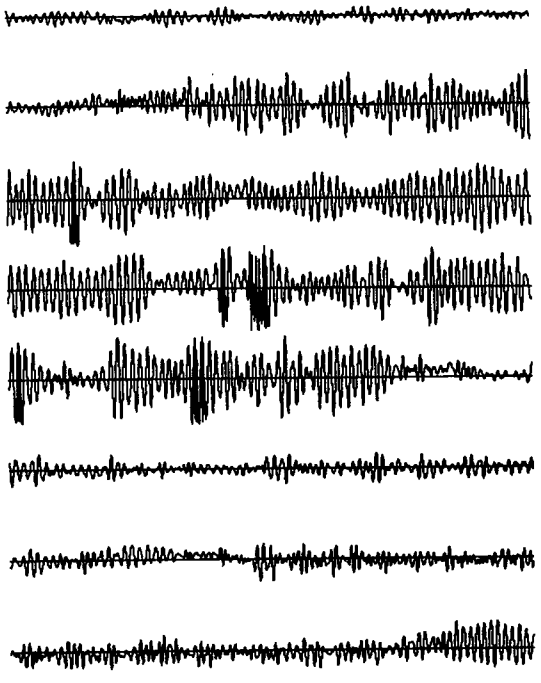

Fig. 7 — Ship roll history from the USS *Providence* (CLG-6), February 14, 1972

Another assumption frequently made is that the process is Gaussian. This assumption, coupled with that of stationarity, implies that the process may be completely characterized by the lower moments of its probability distributions, which include the mean and autocovariance function or, equivalently, the power spectrum. If the process is not Gaussian, the lower moments are no longer the only relevant statistical properties; they are, however, as pointed out by Blackman and Tukey [29], usually the most useful ones.

Power Spectrum of the Process

The autocovariance function of the roll process, assuming stationarity of $\{\Phi(t)\}$, is defined by

$$\gamma(\Phi;u) = E\{[\Phi(t) - \mu][\Phi(t+u) - \mu]\} \tag{16}$$

where E denotes expectation, μ is the mean of the process, and u is the lag. The notation $\gamma(\Phi;u)$, as pointed out previously, indicates that this is the autocovariance γ for the roll process $\{\Phi(t)\}$ and is a function of the lag u.

This function has played a dominant role in the spectral analysis of stationary time series. There have been several reasons for this, but chief among them has been its relationship to the power spectrum of the process $\Gamma(\Phi;f)$ through the Fourier transform

$$\Gamma(\Phi;f) = \int_{-\infty}^{\infty} \gamma(\Phi;u)e^{-i2\pi fu}\, du, \tag{17}$$

a relation attributed to Wiener [20] and Khintchine [21] and referred to as the Wiener-Khintchine theorem.

Power-Spectral Estimators

Since the amount of roll data $\varphi(t)$ available from measurements will, in practice, be limited to some finite interval $(0,T)$, the autocovariance function in Eq. (16) must be estimated by a sample autocovariance function $c(\varphi;u)$:

$$c(\varphi;u) = \begin{cases} \dfrac{1}{T} \displaystyle\int_0^{T-|u|} [\varphi(t) - \bar{\varphi}][\varphi(t + |u|) - \bar{\varphi}]\, dt, & |u| \leqslant T \\ \\ 0 \ (|u| > T). \end{cases} \tag{18}$$

where the sample mean $\bar{\varphi}$ is defined by

$$\bar{\varphi} = \frac{1}{T} \int_0^T \varphi(t)\, dt. \tag{19}$$

The estimator in Eq. (18) is asymptotically unbiased, which can be seen by taking its expectation

$$\begin{aligned} E[c(\Phi;u)] &= E\left\{\frac{1}{T} \int_0^{T-|u|} [\Phi(t) - \bar{\Phi}][\Phi(t + |u|) - \bar{\Phi}]\, dt\right\} \\ &= \frac{1}{T} \int_0^{T-|u|} E\left\{[\Phi(t) - \bar{\Phi}][\Phi(t + |u|) - \bar{\Phi}]\right\} dt \\ &= \frac{1}{T} \int_0^{T-|u|} \gamma(\Phi;u)\, dt \\ &= \left(1 - \frac{|u|}{T}\right) \gamma(\Phi;u) \end{aligned} \tag{20}$$

where it has been assumed that the mean $E[\Phi(t)]$ of the process is zero.†

† Use of the capital Φ in Eq. (20) as opposed to the lowercase φ in Eq. (18) is made to draw attention to the fact that $c(\Phi;u)$ is a random variable, whereas $c(\varphi,u)$ is but a single sample function.

The effect on the power spectrum of estimating the autocovariance function accounts for much of the literature on the theory of spectral analysis. If in place of the autocovariance function (Eq. (16)) we insert the sample autocovariance function (Eq. (18)), we obtain the sample power spectrum

$$C(\varphi;f) = \int_{-\infty}^{\infty} c(\varphi;u)e^{-i2\pi fu}\, du. \tag{21}$$

The first moment of this estimator can be written, using Eq. (20), as

$$E[C(\Phi;f)] = \int_{-\infty}^{\infty} \gamma(\Phi;u)\left(1 - \frac{|u|}{T}\right)e^{-i2\pi fu}\, du. \tag{22}$$

It can be seen that in the limit, as the record length tends to infinity, the expectation tends to the power spectrum of the process, that is,

$$\Gamma(\Phi;f) = \lim_{T\to\infty} E[C(\Phi;f)]. \tag{23}$$

Here lies the major difference between the analysis of deterministic signals and stochastic processes. Only for the case of a deterministic signal does the sample power spectrum converge as the length of the sample tends to infinity. For a stochastic process, it is the ensemble average of the sample power spectrum that converges. A graphic example of the nonconvergence of the sample spectrum for white noise is given by Jenkins and Watts [30]. It is shown there how a single sample spectrum for white noise is not constant, as one might suppose, but is characterized by peaks and nulls that are reduced only through the averaging of many sample spectra.

The equivalence between the sample power-spectral estimator in Eq. (21) and the periodogram of Schuster [31], whose distributional properties are reviewed in subsequent sections, can be seen from the following development, which begins with the definition of the periodogram:

$$\begin{aligned} C(\varphi;f) &= \frac{1}{T}\left|\mathcal{F}\{\varphi(t)\}\right|^2 \\ &= \frac{1}{T}\mathcal{F}\{\varphi(t)\}\mathcal{F}^*\{\varphi(t)\} \\ &= \frac{1}{T}\int_0^T \varphi(\xi)e^{-i2\pi f\xi}\, d\xi \int_0^T \varphi(\eta)e^{i2\pi f\eta}\, d\eta \\ &= \frac{1}{T}\int_0^T \int_0^T \varphi(\xi)\,\varphi(\eta)e^{-i2\pi f(\xi-\eta)}\, d\xi d\eta \end{aligned}$$

$$= \int_{-T}^{T} \frac{1}{T} \int_{0}^{T} \varphi(\eta)\,\varphi(\eta + u)\, d\eta\, e^{-i2\pi fu}\, du$$

$$= \int_{-T}^{T} \frac{1}{T} \int_{0}^{T-|u|} \varphi(\eta)\,\varphi(\eta + |u|)\, d\eta\, e^{-i2\pi fu}\, du$$

$$= \int_{-\infty}^{\infty} c(\varphi;u) e^{-i2\pi fu}\, du,$$

which is the sample power-spectra estimator in Eq. (21). In the development $\mathcal{F}\{\varphi(t)\}$ is the Fourier transform of the sample function $\varphi(t)$, which vanishes outside the interval $(0,T)$. The asterisk denotes the complex conjugate. In line 5 of the development the transformation of variables was made corresponding to $u = \xi - \eta$. The limits of the integral in the last line were extended to $\pm\infty$, realizing that the sample autocovariance function $c(\varphi;u)$ vanishes outside the interval $(-T,T)$.

Distribution of Power-Spectral Estimators

To derive the distributional properties of the roll-frequency estimator in subsequent sections we will need the probability distributions for the sample power-spectral estimators. These will be obtained by first considering the probability distributions for the sample power-spectral estimators for a Gaussian white-noise process $\{Z_k\}$, $k = 0,\pm1,\pm2,\pm3,\ldots$, and then synthesizing the sampled process $\{\Phi_k\}$, $k = 0,\pm1,\pm2,\pm3,\ldots$, by using the white-noise process as the input to a linear filter with a transfer function satisfying the relation

$$|H(f)|^2 = \frac{1}{\sigma^2 \Delta t}\, \Gamma(\Phi_k;f)$$

where σ^2 is the variance of the white-noise process and Δt is the time interval between adjacent measurements (i.e., between Z_k and Z_{k+1}).

The derivation, with some modifications, follows that given by Jenkins and Watts [30]. We consider, then, a sample ($k = 0,\ 1,\ 2,\ldots,N-1$) from the Gaussian white-noise process $\{Z_k\}$, $k = 0,\pm1,\pm2,\ldots$, with zero mean, variance σ^2, and spacing Δt. The sample power-spectral estimator may be written in terms of the periodogram as†

$$C(Z_k;f) = \frac{1}{T} |\mathcal{F}\{Z_k\}|^2, \quad k = 0,1,2,\ldots,N-1 \tag{24}$$

$$= \frac{1}{N\Delta t} \left| \Delta t \sum_{k=0}^{N-1} Z_k e^{-i2\pi fk\Delta t} \right|^2$$

†Sampling of the process in time incurs periodicity in the frequency domain so that the frequency is restricted to the unambiguous range $(-1/2\Delta t, 1/2\Delta t)$, which will be implied for all spectra computed from sampled data.

$$= \frac{\Delta t}{N}\left[\left(\sum_{k=0}^{N-1} Z_k \cos 2\pi fk\Delta t\right)^2 + \left(\sum_{k=0}^{N-1} Z_k \sin 2\pi fk\Delta t\right)^2\right]$$

$$= \frac{\Delta t}{N}\left[A^2(f) + B^2(f)\right] \tag{25}$$

where

$$A(f) = \sum_{k=0}^{N-1} Z_k \cos 2\pi fk\Delta t, \tag{26}$$

$$B(f) = \sum_{k=0}^{N-1} Z_k \sin 2\pi fk\Delta t. \tag{27}$$

Since $E[Z_k] = 0$, then $E[A(f)] = E[B(f)] = 0$, and at the harmonic frequencies $f_n = n/T = n/(N\Delta t)$, $n = 0,1,2,\ldots,N-1$:

$$\mathrm{Var}[A(f_n)] = E[A^2(f_n)]$$

$$= \sigma^2 \sum_{k=0}^{N-1} \cos^2\left(\frac{2\pi nk}{N}\right)$$

$$= \begin{cases} \sigma^2 N, & n = 0, \dfrac{N}{2} \\ \sigma^2 \dfrac{N}{2}, & n = 1,2,\ldots,\dfrac{N}{2}-1. \end{cases} \tag{28}$$

Similarly,

$$\mathrm{Var}[B(f_n)] = \begin{cases} 0, & n = 0, \dfrac{N}{2} \\ \sigma^2 \dfrac{N}{2}, & n = 1,2,\ldots,\dfrac{N}{2}-1, \end{cases} \tag{29}$$

$$\mathrm{Cov}[A(f_n), A(f_m)] = \sum_{k=0}^{N-1}\sum_{l=0}^{N-1} E[Z_k Z_l] \cos\left(\frac{2\pi nk}{N}\right) \cos\left(\frac{2\pi ml}{N}\right)$$

$$= \sigma^2 \sum_{k=0}^{N-1} \cos\left(\frac{2\pi nk}{N}\right) \cos\left(\frac{2\pi nk}{N}\right)$$

$$= 0, \quad n \neq m. \tag{30}$$

Similarly,

$$\mathrm{Cov}[B(f_n), B(f_m)] = 0, \quad n \neq m \tag{31}$$

$$\mathrm{Cov}[A(f_n), B(f_m)] = 0, \quad \text{all } n,m. \tag{32}$$

Since $A(f_n)$ and $B(f_n)$ are linear functions of Gaussian random variables, they are themselves distributed normally. In addition, they are independent, which follows from their being uncorrelated, normal, random variables. Therefore

$$\left.\begin{aligned} \frac{A^2(f_n)}{\mathrm{Var}[A(f_n)]} &= \frac{2A^2(f_n)}{N\sigma^2} \\ \frac{B^2(f_n)}{\mathrm{Var}[B(f_n)]} &= \frac{2B^2(f_n)}{N\sigma^2} \end{aligned}\right\} = \chi_1^2. \tag{33}$$

Since these random variables are independent and distributed as χ_1^2, their sum

$$\frac{2}{N\sigma^2}\left[A^2(f_n) + B^2(f_n)\right] = \frac{2C(Z_k;f_n)}{\sigma^2 \Delta t} = \chi_2^2 \tag{34}$$

is distributed as chi squared with two degrees of freedom except for $n = 0, N/2$, for which $B(f_n) = 0$, so that the sum is chi squared with one degree of freedom.

Since the expectation and variance of a chi-squared random variable with ν degrees of freedom are ν and 2ν, respectively, we can solve for the expectation and variance of the sample power-spectral estimator as follow:

$$E\left[\frac{2C(Z_k;f_n)}{\sigma^2 \Delta t}\right] = 2,$$

$$E[C(Z_k;f_n)] = \sigma^2 \Delta t = \Gamma(Z_k;f_n), \tag{35}$$

$$\mathrm{Var}\left[\frac{2C(Z_k;f_n)}{\sigma^2 \Delta t}\right] = 4,$$

$$\mathrm{Var}[C(Z_k;f_n)] = \sigma^4 \, (\Delta t)^2 = \Gamma^2 \, (Z_k;f_n) \tag{36}$$

where it will be remembered that $\Gamma(Z_k;f)$ is the power spectrum of the process. This shows, as Slutsky [32] stated, that the variance of the sample power-spectral estimator is a constant, independent of the length N, and that, therefore, there is no convergence of the sample power spectrum to the power spectrum of the process as N tends to infinity. Although the derivation above assumed that the noise was Gaussian, the restriction is not severe since the central limit theorem should render the distribution of the random variables $A(f)$ and

$B(f)$ nearly Gaussian and that of the power-spectral estimator nearly chi squared regardless of the distribution of the process.

The analysis of the white-noise process can be extended to the case of white noise as the input to a linear filter, where, by a suitable choice of the transfer function, the power spectrum of any stochastic process can be reproduced. The general relation between the input and output power spectra for a linear system may be written in this case as

$$\Gamma(\Phi_k;f) = |H(f)|^2\,\Gamma(Z_k;f) \tag{37}$$

where for white noise $\Gamma(Z_k;f) = \sigma^2\Delta t$.

The sample power spectrum for a finite segment of the stochastic process may be written

$$C(\Phi_k;f) = \frac{1}{T}\left|\mathcal{F}\left\{\text{rect}\left[\frac{k-(N/2)}{N}\right]\Phi_k\right\}\right|^2$$

$$= \frac{1}{T}\left|\mathcal{F}\left\{\text{rect}\left[\frac{k-(N/2)}{N}\right][h_k * Z_k]\right\}\right|^2 \tag{38}$$

$$\approx \frac{1}{T}\left|\mathcal{F}\left(h_k * \left\{\text{rect}\left[\frac{k-(N/2)}{N}\right]Z_k\right\}\right)\right|^2 \tag{39}$$

$$\approx \frac{1}{T}\left|\mathcal{F}\{h_k\}\,\mathcal{F}\left\{\text{rect}\left[\frac{k-(N/2)}{N}\right]Z_k\right\}\right|^2$$

$$\approx |H(f)|^2\,\frac{1}{T}\left|\mathcal{F}\left\{\text{rect}\left[\frac{k-(N/2)}{N}\right]Z_k\right\}\right|^2$$

$$\approx |H(f)|^2\,C(Z_k;f) \tag{40}$$

where, because we know the distribution of the sample power-spectral estimator $C(Z_k;f)$ for the white-noise process, we may write

$$E[C(\Phi_k;f)] \approx |H(f)|^2\,\Gamma(Z_k;f) = \Gamma(\Phi_k;f). \tag{41}$$

Similarly, as seen from Eq. (35), $C(Z_k;f)$ is an unbiased estimator.

$$\text{Var}[C(\Phi_k;f)] \approx \Gamma^2(\Phi_k;f). \tag{42}$$

Jenkins and Watts [30] point out that the approximation in going from Eq. (38) to Eq. (39) requires that the impulse response $h(t)$ tend to zero in a time short compared with the length T of the sample. The reason for this can, perhaps, be better appreciated by a comparison of the spectra in each case. Evaluating the transform within the modulus signs for Eq. (38) gives

$$T\,\text{sinc}(Tf)e^{-i\pi Tf} * [H(f)Z(f)] \tag{43}$$

and for Eq. (39),

$$H(f)[T\ \mathrm{sinc}(Tf)e^{-i\pi Tf} * Z(f)] \tag{44}$$

where $H(f)$ and $Z(f)$ are the Fourier transforms of $h(t)$ and $\{Z_k\}$ for $k = 0,1,2,\ldots,N-1$. In Eq. (43) we see that the smoothing and consequent leakage through the sidelobes of the sinc-function spectral window corresponding to the rect-function data window is applied to the transfer function as well as to the noise, whereas in Eq. (44) the same effects are applied only to the noise, and not to the transfer function. From this formulation it is easy to see that the spectral window would have to be narrow (large sample length T) relative to the resonant bandwidth of the transfer function in order for the approximation to be close.

Stability of Power-Spectral Estimators

The defect in the periodogram relating to its nonconvergence for increasing sample size was known to Schuster [31], who commented that, were it not for the prohibitive computational effort required, one should follow the practice, common in optics, of averaging the successive periodograms obtained by varying continuously the starting time of the sample. "Smoothing" of the periodogram by averaging over neighboring values of frequency was suggested by Daniell [33]. Kendall [34] then observed that this smoothing was tantamount to truncating the autocorrelation function, whose Fourier transform had been noted by Wiener [20] to be equivalent to the periodogram. A similar result was arrived at independently by Bartlett [35], who noticed that averaging periodograms obtained from contiguous lengths of series was approximately equivalent to truncating the correlogram (autocorrelation function) at a point represented by the length of the subseries.

To appreciate the reduction in the variance (increase in stability) achieved by averaging sample spectra, we need only consider that the distribution of the sample power-spectral estimators for Gaussian white noise derived in the preceding section was chi squared with two degrees of freedom except for $n = 0, N/2$, where the estimators were distributed as chi squared with one degree of freedom. By the reproductive property of chi-squared random variables with ν degrees of freedom, the distribution of the sum of m such independent random variables is also chi squared but with νm degrees of freedom. Therefore, if we define

$$\overline{C}(Z_k;f_n) = \frac{1}{m}\sum_{i=1}^{m} C_i(Z_k;f_n) \tag{45}$$

where $\overline{C}(Z_k;f_n)$ is the smoothed sample power-spectral estimator obtained by averaging m sample power-spectral estimators and where $C_i(Z_k;f_n)$ is the sample power-spectral estimator computed from the ith nonoverlapping sample of the process $\{Z_k\}$, we may write

$$\frac{2m\bar{C}(Z_k;f_n)}{\sigma^2\Delta t} = \begin{cases} \chi^2_{2m}, & n = 1,2,\ldots,\dfrac{N}{2}-1 \\ \chi^2_m, & n = 0,\dfrac{N}{2}. \end{cases}$$

The variance of the smoothed power-spectral estimate is then

$$\mathrm{Var}\left[\frac{2m\bar{C}(Z_k;f_n)}{\sigma^2\Delta t}\right] = 4m,$$

$$\mathrm{Var}[\bar{C}(Z_k;f_n)] = \frac{\sigma^4(\Delta t)^2}{m} = \frac{\Gamma^2(Z_k;f_n)}{m}, \tag{46}$$

which shows that the variance of the smoothed sample power-spectral estimators for Gaussian white noise has decreased by a factor of $1/m$ by averaging m sample spectra.

Use of the above results and Eq. (40) allows us to derive an expression for the variance of the smoothed sample power-spectral estimator for an arbitrary stochastic process where the sample length T is large. Taking the m-fold average of both sides of Eq. (40), we obtain

$$\bar{C}(\Phi_k;f_n) \approx |H(f_n)|^2\bar{C}(Z_k;f_n),$$

$$\frac{2m\bar{C}(\Phi_k;f_n)}{|H(f_n)|^2\,\sigma^2\Delta t} \approx \frac{2m\bar{C}(Z_k;f_n)}{\sigma^2\Delta t} = \chi^2_{2m}, \tag{47}$$

$$\mathrm{Var}\left[\frac{2m\bar{C}(\Phi_k;f_n)}{|H(f_n)|^2\,\sigma^2\Delta t}\right] \approx 4m,$$

$$\mathrm{Var}[\bar{C}(\Phi_k;f_n)] \approx \frac{|H(f_n)|^4(\Delta t)^2\,\sigma^4}{m}$$

$$\approx \frac{|H(f_n)|^4\;\Gamma^2(Z_k;f_n)}{m}$$

$$\approx \frac{\Gamma^2(\Phi_k;f_n)}{m}. \tag{48}$$

Given a record of finite length, this smoothing procedure suggests that it be subdivided into m segments each T seconds long. The larger m is, the smaller the variance will be. However, as m increases, T decreases, resulting in a larger bias $B(f)$, given by

$$B(f) = E[\bar{C}(\Phi_k;f)] - \Gamma(\Phi_k;f). \tag{49}$$

Bias of Power-Spectral Estimators

To understand the source of the bias and its relationship to the variance of the smoothed sample power-spectral estimators for a record of given length that has been partitioned into m segments, we will redefine the sample autocovariance function given by Eq. (18). For clarity continuous time functions will be assumed since discreteness in time implies periodicity in the spectrum, which we wish, for the present, to avoid. For continuous time the sample autocovariance function is given by Eq. (18) as

$$c(\varphi;u) = \frac{1}{T}\int_0^{T-|u|} [\varphi(t) - \bar{\varphi}][\varphi(t + |u|) - \bar{\varphi}]\, dt.$$

If we suitably restrict the factors in the integrand with rectangle functions

$$\operatorname{rect}\left(\frac{t}{T}\right) = \begin{cases} 1, & |t| \leqslant \dfrac{T}{2}, \\ 0, & \text{otherwise}, \end{cases} \tag{50}$$

we can write the limits of the integral as extending from $-\infty$ to $+\infty$:

$$c(\varphi;u) = \frac{1}{T}\int_{-\infty}^{\infty} \operatorname{rect}\left[\frac{t - (T/2)}{T}\right][\varphi(t) - \bar{\varphi}]\operatorname{rect}\left[\frac{t - (T/2) + |u|}{T}\right]$$

$$\times [\varphi(t + |u|) - \bar{\varphi}]\, dt. \tag{51}$$

Taking the expectation of both sides and assuming a process with zero mean $E[\Phi] = \mu_\varphi = 0$, we obtain

$$E[c(\Phi;u)] = \frac{1}{T}\int_{-\infty}^{\infty} \operatorname{rect}\left[\frac{t - (T/2)}{T}\right]\operatorname{rect}\left[\frac{t - (T/2) + |u|}{T}\right]$$

$$\times E\left\{[\Phi(t) - \bar{\Phi}][\Phi(t + |u|) - \bar{\Phi}]\right\} dt$$

$$= \frac{1}{T}\int_{-\infty}^{\infty} \operatorname{rect}\left[\frac{t - (T/2)}{T}\right]\operatorname{rect}\left[\frac{t - (T/2) + |u|}{T}\right]\gamma(\Phi;u)\, dt$$

$$= \frac{1}{T}\int_{-\infty}^{\infty} \operatorname{rect}\left[\frac{t - (T/2)}{T}\right]\operatorname{rect}\left[\frac{t - (T/2) + |u|}{T}\right] dt\ \gamma(\Phi;u),$$

$$= \left(1 - \frac{|u|}{T}\right)\gamma(\Phi;u), \tag{52}$$

which is Eq. (20). With this formulation we recognize that the use of the rectangular data window to truncate the time series $\{\Phi(t)\}$ in Eq. (51) is equivalent to the use of the triangular lag window to weight the autocovariance function of the process. We note also from Eq. (52) that the triangular lag window results from the autocorrelation, or self-convolution (since the two operations are identical for even functions), of the rectangular data window. This suggests, with some malice aforethought, that we weight the data with a window appropriate to the nature of the process and of the information being sought. If, then, we define as the sample autocovariance function (assuming zero mean for the process)

$$c(\varphi;u) = \frac{1}{T}\int_{-\infty}^{\infty} w\left[\frac{t-(T/2)}{T}\right]\varphi(t)w\left[\frac{t-(T/2)+|u|}{T}\right]\varphi(t+|u|)\,dt \tag{53}$$

where the data window $w(t)$ has the properties

$$w(0) = 1, \tag{54a}$$

$$w(t) = w(-t), \tag{54b}$$

$$w(t) = 0, \quad |t| > \frac{1}{2}, \tag{54c}$$

we can derive the expression for the expectation of the smoothed sample power-spectral estimator:

$$E[\bar{c}(\Phi;u)] = E\left[\frac{1}{m}\sum_{k=1}^{m} c_k(\Phi;u)\right]$$

$$= \frac{1}{m}\sum_{k=1}^{m}\frac{1}{T}\int_{-\infty}^{\infty} w\left[\frac{t-(T/2)-kT}{T}\right] w\left[\frac{t-(T/2)-kT+|u|}{T}\right]$$

$$\times E[\Phi(t-kT)\Phi(t-kT+|u|)]\,dt$$

$$= \gamma(\Phi;u)\,\frac{1}{m}\sum_{k=1}^{m}\frac{1}{T}\int_{-\infty}^{\infty} w\left[\frac{t-(T/2)-kT}{T}\right] w\left[\frac{t-(T/2)-kT+|u|}{T}\right] dt.$$

On Fourier transforming both sides, we obtain

$$\mathcal{F}\{E[\bar{c}(\Phi;u)]\} = \mathcal{F}\left\{E\left[\frac{1}{m}\sum_{k=1}^{m} c_k(\Phi;u)\right]\right\},$$

$$E[\mathcal{F}\{\bar{c}(\Phi;u)\}] = \Gamma(\Phi;f) * \frac{1}{m}\sum_{k=1}^{m} T|W(Tf)e^{-i2\pi fkT}|2$$

$$= \Gamma(\Phi;f) * \frac{1}{m} \sum_{k=1}^{m} TW^2(Tf),$$

$$E[(\bar{C}(\Phi;f)] = \Gamma(\Phi;f) * TW^2(Tf). \tag{55}$$

From Eq. (55) we see that the effect of truncating the process to a length T with a data window $w\{[t - (T/2)]/T\}$ is the convolution of the power spectrum $\Gamma(\Phi;f)$ of the process with the spectral window $TW^2(Tf)$. In general, if we knew nothing about the spectrum of the process, the possibility of mischief inherent in the convolution of the spectrum we are endeavoring to estimate, with a spectral window having a finite bandwidth and a sidelobe structure of finite extent, would give us little cause for confidence in an estimate of the position of a peak in the spectrum.

Variance of the Roll-Frequency Estimator

If the sample length T is large enough for us to assume that the sample power-spectral estimate is essentially unbiased, then it should be possible to assess the effect of the variability of the smoothed sample power-spectral estimates on the variance of the estimate of the resonant frequency, or peak of the transfer function, when Gaussian white noise is the input. For the small values of roll damping that normally obtain, the resonant frequency will be the natural roll frequency, as noted on pp. (12 - 13).

A sketch of the procedure is shown in Fig. 8. The power spectrum of the process $\Gamma(\Phi_k;f)$ is obtained by putting Gaussian white noise $\{Z_k\}$ with variance σ^2 through a filter with the transfer function $H(f)$ given by Eq. (4). Spaced at intervals of $\Delta f = T^{-1}$ along the spectrum $\Gamma(\Phi_k;f)$ are circles marking the mean value of the independent spectral estimates. Superimposed on the spectrum at one of these positions is the chi-squared probability density function that gives the variability of the corresponding spectral estimate.

The sample power-spectral estimators at the harmonic frequencies $f_n = n\Delta f$ can be shown to be independent, by an argument similar to that given on pp. (22 - 24). Briefly, the coefficients $A(f_n)$ are shown to be independent of the coefficients $A(f_m)$ for $n \neq m$ not only within a given sample spectrum but from spectrum to spectrum in the collection of spectra over which the average is to be taken. A similar argument holds for $B(f_n)$ and $B(f_m)$ as well as for $A(f_n)$ and $B(f_m)$ for all n. The average power-spectral estimator at the frequency f_n is then simply a function (a weighted sum of squares) of random variables that are independent of the corresponding random variables at all other frequencies f_m, $n \neq m$; and since functions of independent random variables are independent, the desired result follows.

The probability density function for the smoothed sample power-spectral estimators is derived as follows. If the random variable x is distributed as chi squared with ν degrees of freedom, we may write its probability density function $p_X(x)$ as

$$p_X(x) = \frac{1}{2^{\nu/2}\Gamma(\nu/2)} x^{(\nu-2)/2} e^{-x/2} U(x)$$

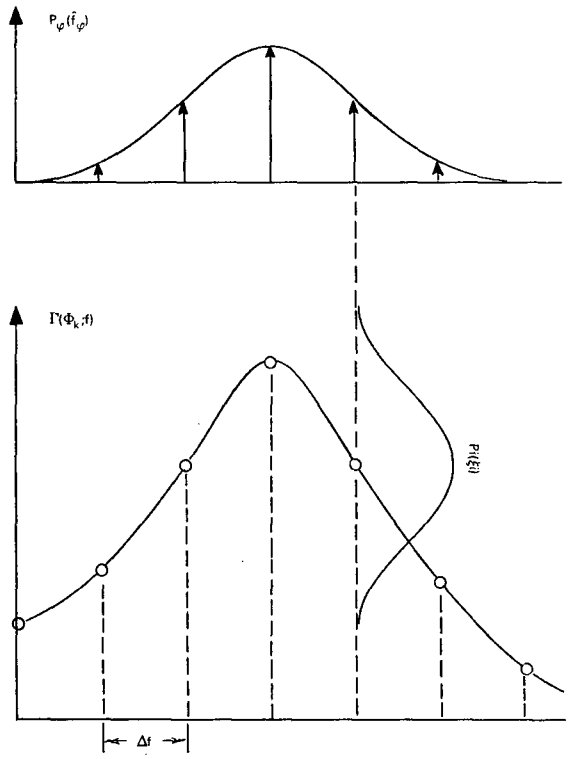

Fig. 8 — Construction showing transformation of probability density function from spectral estimate to roll-frequency estimate

where Γ is the gamma function and $U(x)$ is the unit step function. For $\nu = 2m$, corresponding to the averaging of m such independent random variables,

$$p_X(x) = \frac{1}{2^m \Gamma(m)} x^{m-1} e^{-x/2} U(x).$$

For $y = ax$,

$$p_Y(y) = \frac{1}{|a|} p_X\left(\frac{y}{a}\right)$$

$$= \frac{1}{a^m 2^m \Gamma(m)} y^{m-1} e^{-y/2a} U(y). \tag{56}$$

If we set $|H(f_n)|^2 \sigma^2 \Delta t = \Gamma(\Phi_k; f_n)$, we have, from Eq. (47) for the above transformation

$$x = \frac{2m}{\Gamma(\Phi_k; f_n)} \bar{C}(\Phi_k; f_n) = \chi^2_{2m},$$

$$y = \bar{C}(\Phi_k; f_n),$$

$$a = \frac{\Gamma(\Phi_k; f_n)}{2m}.$$

Substitution of these equations into Eq. (56) yields†

$$p_n(\xi_n) = \frac{m^m}{\Gamma^m(\Phi_k; f_n)\Gamma(m)} \xi_n^{m-1} \exp\left[\frac{-m\xi_n}{\Gamma(\Phi_k; f_n)}\right] U(\xi_n). \tag{57}$$

In Fig. 8 there is plotted above the spectrum with the superimposed probability density function of Eq. (57) the probability (a discrete density function) that a given independent spectral estimate at frequency f_i is the global maximum in the smoothed power spectrum and therefore interpretable as the peak of the transfer function. The probability that $\bar{C}(\Phi_k; f_i)$ is the global maximum in the smoothed sample power spectrum may be written

$$P\{\xi_i = \max[\xi_j, j=1,2,\ldots,N]\}$$

$$= \int_0^\infty d\xi_i \int_0^{\xi_i} \int_0^{\xi_i} \cdots \int_0^{\xi_i} p_{1,2,\ldots,N}(\xi_1, \xi_2, \ldots, \xi_N)$$

$$\times d\xi_1\, d\xi_2 \ldots d\xi_{i-1}\, d\xi_{i+1} \ldots d\xi_N. \tag{58}$$

Since the ξ_j terms constitute independent spectral estimates for the assumed conditions, we may write

$$P\{\xi_i = \max[\xi_j, j=1,2,\ldots,N]\}$$

$$= \int_0^\infty d\xi_i\, p_i(\xi_i) \prod_{\substack{j=1 \\ j\neq i}}^{N} \int_0^{\xi_i} d\xi_j p_j(\xi_j) \tag{59}$$

where the probability density functions are given by Eq. (57). If we make use of the integral formula [36]

$$\int x^m e^{ax}\, dx = e^{ax} \sum_{r=0}^{m} (-1)^r \frac{m! x^{m-r}}{(m-r)! a^{r+1}}, \tag{60}$$

the integrals in Eq. (59) can be expressed as a finite sum:

$$\int_0^{\xi_i} d\xi_j\, p_j(\xi_j) = 1 - \exp\left[-\frac{m\xi_j}{\Gamma(\Phi_k; f_j)}\right] \sum_{n=1}^{m} A_{n,j} \xi_j^{m-n} \tag{61}$$

† For simplicity of notation we set $\xi_n = \bar{C}(\Phi_k; f_n)$.

where the summation coefficient $A_{n,j}$ is given by

$$A_{n,j} = \left[\frac{m}{\Gamma(\Phi_k; f_j)}\right]^{m-n} \frac{1}{\Gamma(m - n + 1)}. \tag{62}$$

The probability density function for the roll-frequency estimator $\hat{f}_\varphi$, the frequency of the peak in the smoothed sample power spectrum, may then be written

$$P_\varphi(\hat{f}_\varphi) = \sum_{i=1}^{N} \delta(\hat{f}_\varphi - f_i) \int_0^\infty d\xi_i \, p_i(\xi_i) \prod_{\substack{j=1 \\ j\neq i}}^{N} \int_0^{\xi_i} d\xi_j \, p_j(\xi_j) \tag{63}$$

where the probability density functions are given by Eq. (57).

The integral in Eq. (63) was evaluated for several values of m, the number of spectra averaged. The envelope of the resulting discrete distributions is plotted in Fig. 9. For the purpose of the plot, the frequency was transformed to fractional error ϵ according to

$$\epsilon = \frac{f_\varphi - \hat{f}_\varphi}{f_\varphi}$$

where f_φ is the natural roll frequency and $\hat{f}_\varphi$ is the estimate. The slight asymmetry of the envelopes near the peak is due to the coarseness of the frequency intervals taken, in this case 0.0002 Hz, relative to the spread in the distribution.

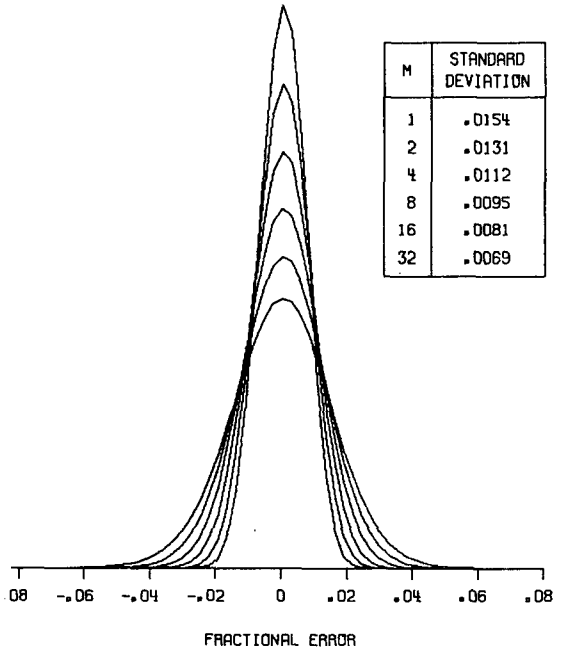

Fig. 9 — Probability density functions for the fractional error in the estimated resonant frequency for simulated still-water rolling with number of spectra averaged

Several aspects of the behavior of these distributions are worthy of note. First, the reduction in the variance due to averaging is seen to be less than $1/m$ even though, as noted from Eq. (48), the variance in the spectral estimates themselves is reduced by $1/m$. If the standard deviation for $m = 1$ were taken as the deviation of the population, the standard deviation for $m = 16$ would be 0.0039 rather than 0.0081.

Second, the probability density functions appear to be Gaussian, which is confirmed by plotting their cumulative distribution functions on normal probability paper, as shown in Fig. 10 for $m = 8$. This is interesting because a moment's reflection about the nature of the transformation in Fig. 8 appears to indicate that the resulting probability density function would be dependent on the shape of the spectrum $\Gamma(\Phi_k; f)$. To check the shape dependence, we made the transformation for $m = 1$ and a roll-damping coefficinet $\kappa = 0.256$. The spectrum (transfer function) for this case is seen from Fig. 2 to be somewhat more asymmetrical. The asymmetry in this case was reflected in the tails of the probability density function, which decreased at unequal rates, the one on the left dying out more slowly. However, due apparently to the high degree of symmetry in the resonant peak in the vicinity of resonance and the fact that most of the probability is contributed by this vicinity, the resulting distribution is, to first order, symmetrical.

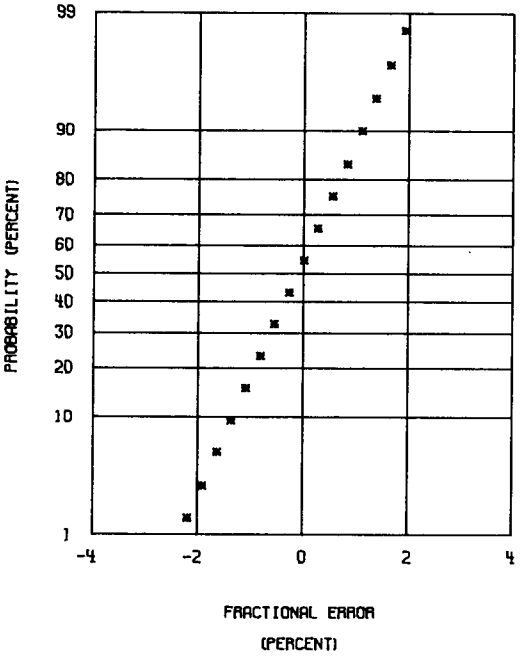

Fig. 10 — Cumulative distribution function for the fractional error in the estimated resonant frequency for simulated still-water rolling

The transfer function was next multiplied by the Pierson-Moskowitz wave-slope spectra [16] for windspeeds in excess of 20 m/sec to obtain simulated roll spectra, and the above

transformation of probability density functions was made. Although the simulated spectra differ for rolling in still water and rolling in Pierson-Moskowitz seas, identical results were obtained; this appears to be explained by the argument above regarding the high degree of symmetry in the resonant peak.

Bias of the Roll-Frequency Estimator

In the case at hand, where we are seeking limited information about the power spectrum and hence the system — that is, the position of the peak of the transfer function — we are not entirely without hope in assessing the effect of bias due to a finite sample length. For example, if the peak in the power spectrum were symmetrical and it were possible to eliminate any other asymmetry, then the bandwidth and sidelobe structure of the spectral window, though contributing to bias in the measurement of power at a particular frequency, would leave the position of the peak unaltered in the sample power spectrum.

We are fortunate in the case of the roll spectrum since, as examination of Fig. 2 will reveal, there is considerable symmetry in the transfer function. It would be of interest to examine the effect of the convolution in Eq. (55), which is the cause of bias in the sample power-spectral estimator, on the position of the single spectral peak, assuming for the roll spectrum the squared modulus of the transfer function in Eq. (4). Extension of the analysis to a ship at sea could be made by assuming the roll spectrum to be the product of the squared modulus of the transfer function in Eq. (4) and the wave-slope frequency spectrum in Eq. (14) obtained from the Pierson-Moskowitz [16] spectrum in Eq. (13).

We will examine first the case of white noise applied to the input of a linear filter whose transfer function is that given by Eq. (4). Assuming a noise process having unit variance, we may write the power spectrum of the output of the filter as

$$\Gamma(\Phi_k;f) = \left\{\left[1 - \left(\frac{f}{f_r}\right)^2\right]^2 + 4\kappa^2 \left(\frac{f}{f_r}\right)^2\right\}^{-1} \tag{64}$$

where $\kappa = 0.032$ Hz and $f_r = 0.0731$ Hz, corresponding to the values assumed for the USS *Providence*. If we assume that the output of the filter is truncated to a length T by a data window, Eq. (55) becomes

$$E[\overline{C}(\Phi_k;f)] = \left\{\left[1 - \left(\frac{f}{f_r}\right)^2\right]^2 + 4\kappa^2\left(\frac{f}{f_r}\right)^2\right\}^{-1} * TW^2(Tf). \tag{65}$$

We wish to estimate the frequency of the resonant peak in the spectrum — the frequency that, in the absence of bias, we saw from Eq. (5) to be equal to 0.0730 Hz and that, for the small values of the roll-damping coefficient that normally obtain, may be taken as the roll-frequency estimator $\hat{f}_\varphi$. The results of the convolution in Eq. (65) are summarized in Table 1, which shows for various truncation lengths T the roll-frequency estimator $\hat{f}_\varphi(T)$ and the bias $B(T)$ in the estimate, both as functions of the truncation length. For this case of a driving function with a uniform spectrum, the bias is seen to vanish for truncation lengths greater than 100 sec, which is of the order of the decorrelation time

Table 1 — Bias of Roll-Frequency Estimator Resulting From Finite Sample Length for Simulated Rolling in Still Water

T (sec)	$\hat{f}_\varphi(T)$ (Hz)	$B(T)$* (Hz)
10	0.0718	-0.0012
20	0.0724	-0.0006
30	0.0728	-0.0002
40	0.0728	-0.0002
50	0.0729	-0.0001
60	0.0729	-0.0001
70	0.0729	-0.0001
80	0.0729	-0.0001
90	0.0729	-0.0001
100	0.0730	-0.0000

*$B(T) = \hat{f}_\varphi(T) - f_\varphi$.

of the roll process. The roll-frequency estimator is shifted down in frequency because of the particular asymmetry in the tails of the transfer function; that is to say, more power leaks in through the sidelobes of the spectral window from the transfer function below resonance and from the negative-frequency image (the mirror image of the curves in Fig. 2) than from the transfer function above resonance, where the power drops off more rapidly.

In Table 2 the power transfer function has been multiplied by wave-slope spectra derived from Pierson-Moskowitz spectra [16] for windspeeds from 20 to 50 m/sec. The bias is seen to be larger and shifted even more than before to lower values. There are two causes for the increased bias. First, there is increased leakage through the sidelobes of the spectral window. Second, there is a shift in the position of the peak that results from the steepness in the spectrum of the driving force in the vicinity of resonance. Bias resulting from the latter cause was investigated; the results are summarized in Table 3, which shows the position of the resonant peak in the simulated roll spectrum when the spectral window is the delta function, or identity operator under convolution. Comparison of Table 3 and Fig. 3 shows that the resonant frequency is shifted toward the peak of the wave-slope spectrum, as one would expect. Also to be noted is the small contribution to the bias from this cause, the major contributor being leakage through the sidelobes of the spectral window.

The resonant peak of the transfer function is completely obliterated as a result of the steepness of the wave-slope spectrum in the vicinity of resonance of windspeeds lower than about 15 m/sec. This seems incongruous with the results discussed in the next section, where well-defined resonant peaks obtained for windspeeds in this range. The Pierson-Moskowitz spectra for low windspeeds have little energy at the frequencies corresponding to roll resonance for most large ships. However, the oceans are normally characterized by the presence of swell at these frequencies — swell that, as Kinsman [37] pointed out,

Table 2 — Bias of Roll-Frequency Estimator Resulting From Finite Sample Length for Simulated Rolling Among Waves* at a Windspeed of 20 to 50 m/sec

T (sec)	$\hat{f}_\varphi(T)$ (Hz)	$B(T)$† (Hz)
10	0.0681	-0.0049
20	0.0697	-0.0033
30	0.0715	-0.0015
40	0.0719	-0.0011
50	0.0721	-0.0009
60	0.0723	-0.0007
70	0.0724	-0.0006
80	0.0725	-0.0005
90	0.0725	-0.0005
100	0.0726	-0.0004
∞	‡	

*Pierson-Moskowitz spectrum [16].
†$B(T) = \hat{f}_\varphi(T) - f_\varphi$.
‡See Table 3.

Table 3 — Bias of Roll-Frequency Estimator Resulting From Steepness of Driving-Force Spectrum*

V (m/sec)	$\hat{f}_\varphi(V)$ (Hz)	$B(V)$ (Hz)
5	Resonant peak obliterated	
10	Resonant peak obliterated	
15	0.0733	0.0003
20	0.0731	0.0001
25	0.0731	0.0001
30	0.0730	0.0000
35	0.0730	0.0000
40	0.0730	0.0000
45	0.0730	0.0000
50	0.0730	0.0000

*Derived from Pierson-Moskowitz spectrum [16].

travels with very little attenuation from the storm centers where it is generated to distant points on the ocean's surface. In deducing the form of the Pierson-Moskowitz spectrum, the authors first had to cull our all those wave-height spectra "contaminated" by swell.

APPLICATION OF METHOD TO SHIP ROLL HISTORY

Summary of Experimental Conditions

The ship motion histories treated in this study, with but one exception, were obtained from the Airborne Radar Branch of the Naval Research Laboratory. The exception is the motion history of the USS *John F. Kennedy* (CVA-67) which the author, assisted by F. Fine, obtained with instrumentation on loan from the Airborne Radar Branch. Since, in general, the data was obtained for some other study, there was no control over the experimental conditions.

The instrumentation used to record the data, described in detail by Kremer et al. [38], was connected to the appropriate synchro transmitters (roll, pitch, and heading), which in turn were connected to the ship gyrocompass or fire-control stable element. Data was sampled at a rate of 10 Hz and quantized to 12 bits. The data was recorded in computer-compatible format as two 48-bit words per frame with 1200 frames per record. The format is shown diagrammatically in Fig. 11. The frame marker used to identify the beginning of the frame was to allow unscrambling of the data in those cases where the recorder lost synchronism with the synchro-to-digital converters.

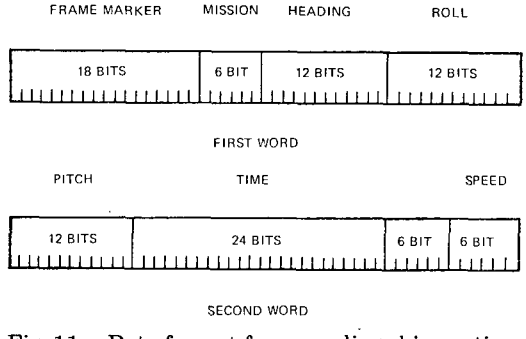

Fig. 11 — Data format for recording ship motion histories on magnetic tape

The ships whose roll histories were analyzed in this study are listed in Table 4 with their size parameters. Measurements were made both en route and in the appropriate operating areas off the coast of southern California and off Norfolk, Virginia. In most cases, the ships executed a box pattern on courses 000, 090, 180, and 270 degrees True and on courses 045, 135, 225, and 315 degrees True. The ship steamed for about 15 min on each leg in turn for a total of 4 hr, thereby executing each leg twice. Table 5 summarizes the conditions of wind and sea that obtained during the recording of the 12-hr roll history for the USS *Providence* that is analyzed in detail in this study.

Table 4 — Summary of Ship-Size Parameters*

Ship Name	Type	Hull Number	Length† (ft)	Beam‡ (ft)	Draft (ft)	Displacement‖ (tons)
Kyes	Destroyer	DD-787	391	41	19	3,500
Shelton	Destroyer	DD-790	391	41	19	3,500
Buckley	Destroyer	DD-808	391	41	19	3,500
Hanson	Destroyer	DD-832	391	41	19	3,500
Parks	Destroyer	DD-884	391	41	19	3,500
Hull	Destroyer	DD-945	418	45	20	4,050
Towers	Guided missile destroyer	DDG-9	432	47	20	4,500
McCain	Guided missile destroyer	DDG-36	493	50	21	5,200
Dahlgren	Guided missile frigate	DLG-12	513	53	25	5,800
Thomaston	Dock landing ship	LSD-28	510	84	19	11,270
Coronado	Amphibious transport dock	LPD-11	570	84	23	16,900
Providence	Guided missile light cruiser	CLG-6	610	66	25	14,600
Kennedy	Attack aircraft carrier	CVA-67	1048	130	36	87,000

*Data from Ref. 39. Conversion factors: 1 ft = 0.3048 m; 1 ton = 907.18474 kg.
†Length measurements rounded to the nearest foot.
‡At waterline.
‖At full load.

Table 5 — Synoptic Observations During Test of USS *Providence**

Time	Wind		Swell		
	Direction (degrees True)	Force (m/sec)	Direction (degrees True)	Period (sec)	Height (m)
1000†	157	7.7	145	3	0.9
1100	170	9.8	145	3	0.9
1200	000	4.1	190	4	1.2
1300	000	4.1	275	4	1.2
1400	000	4.1	280	4	1.2
1500	052	2.6	310	5	1.5
1600	089	3.1	310	6	1.8
1700	128	2.6	295	6	1.8
1800	023	2.1	295	6	1.8
0300‡	292	4.6	090	4	0.6
0400	292	4.6	090	4	0.6
0500	300	4.6	090	4	0.6
0600	320	4.6	090	4	0.6
0700	295	5.1	090	4	0.6

*Ship position 32.7°N, 118.4°W.
†February 14, 1972.
‡February 16, 1972.

Choosing Parameters for the Analysis

In the analysis of ship motion histories we are free to vary the following parameters:

1. The sample length T

2. The sample rate $(\Delta t)^{-1}$

3. The frequency spacing Δf

4. The shape of the data window $w(t)$

5. The number m of spectra that are averaged in determining a single estimate of the roll frequency

6. The total length mT of data entering into a determination of a single estimate of the roll frequency

7. The method of averaging.

The choice of a sample rate is guided by the bandwidth of the data to be analyzed. The classic sampling theorem of Oliver, Pierce, and Shannon [40] requires that a low-pass signal be sampled at a rate at least twice that of the highest frequency present in order to be able to recover the original signal from the samples. To sample at a lower rate would result in distortion of the spectrum as a result of aliasing. In the present case, since we are looking for behavior at a very low frequency, some aliasing in the spectrum could be tolerated so long as the spectrum roll off were steep enough. Figure 12 shows the roll spectrum for 4 hr of data from the USS *Providence*. The spectrum was obtained by averaging 12 spectra (m = 12), each representing 20 min of data (T = 1200 sec). The power density is down by 30 dB at 0.15 Hz, which implies that a sample rate as low as 0.25 Hz might have been used.

The choice of the frequency spacing Δf is dictated by the fineness desired in the measurement of the roll frequency and the variance in its distribution. The frequency spacing is a simple function of the sample rate f_s, which is equal to $(\Delta t)^{-1}$, and the size n of the transform. The fineness in frequency can be obtained by adding zeros to the data to fill out the input array of the transform. We have, then, for the frequency spacing

$$\Delta f = \frac{f_s}{n}.$$

Table 6 lists values of the frequency spacing Δf as a function of some of the sample rates available on the basis of a maximum sample rate of 10 Hz. The use of a low sample rate eases the requirement on the size of the transform for a given frequency spacing. A lower bound on the sample rate and therefore on the size of the transform would be of especial interest in the design of a fast-Fourier-transform device for use aboard a vessel in measuring roll frequency. In the laboratory it would represent a saving in computer time for cases in which large amounts of data must be processed.

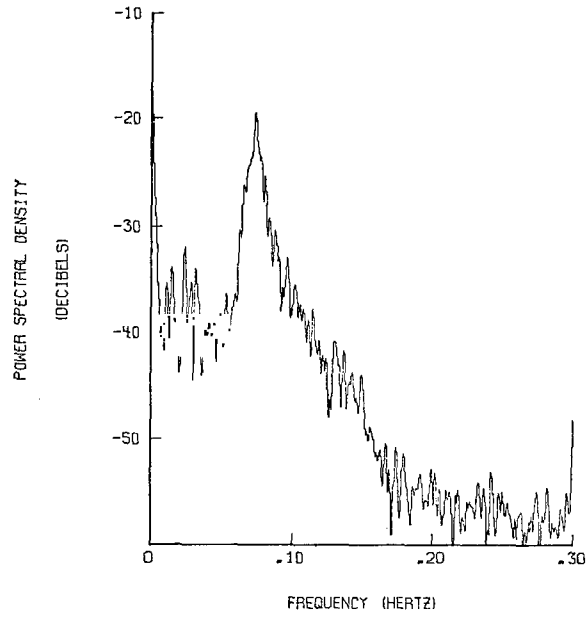

Fig. 12—Power-spectrum estimate for the roll history of the USS *Providence* (CLG-6) (T = 1200 sec, m = 12)

Table 6 — Dependence of the Frequency Spacing Δf on Sample Rate f_s and Transform Size n

Transform Size n	Sample Rate f_s (Hz)					
	10	5	2	1	0.5	0.25
256	0.0391	0.0195	0.0078	0.0039	0.0020	0.0010
512	0.0195	0.0098	0.0039	0.0020	0.0010	0.0005
1024	0.0098	0.0049	0.0020	0.0010	0.0005	0.0002
2048	0.0049	0.0024	0.0010	0.0005	0.0002	0.0001
4096	0.0024	0.0012	0.0005	0.0002	0.0001	
8192	0.0012	0.0006	0.0002	0.0001		

Of the several parameters, the sample length is perhaps most critical to the analysis. For reasons of economy, the sample length should be small. On the other hand. resolution of low-frequency components in the spectrum demands a large sample length. Closely tied to the sample length is the number of spectra that are averaged and therefore the total length of data that enters into the determination of a single estimate of the roll frequency.

An attempt to confirm the optimum relationship among these three parameters is shown in Tables 7 and 8, which present a part of the results of a parametric analysis. Table 7 shows the results of averaging m spectra each computed from T seconds of data. Shown is the mean $\bar{\hat{f}}_\varphi$ of the roll-frequency estimates thus determined, the sample standard

Table 7 — Dependence of the Mean $\bar{\hat{f}}_\varphi$ and the Standard Deviation S_m of the Roll-Frequency Estimates on the Number m of Spectra Averaged*

Number of Average Spectra	mT (sec)	m	$\bar{\hat{f}}_\varphi$ (Hz)	S_m (Hz)	$S_1 m^{-1/2}$ (Hz)
144	100	1	0.0730	0.0071	0.0071
72	200	2	0.0732	0.0046	0.0050
36	400	4	0.0735	0.0033	0.0036
18	800	8	0.0731	0.0016	0.0025
9	1600	16	0.0731	0.0012	0.0018
6	2400	24	0.0730	0.0011	0.0014

*Sample length T = 100 sec.

Table 8 — Dependence of the mean $\bar{\hat{f}}_\varphi$ and the Standard Deviation S_m of the Roll-Frequency Estimates on the Sample Length T*

T (sec)	m	$\bar{\hat{f}}_\varphi$ (Hz)	S_m (Hz)
2400	1	0.0723	0.0017
1200	2	0.0729	0.0018
800	3	0.0725	0.0018
600	4	0.0734	0.0016
480	5	0.0732	0.0016
400	6	0.0725	0.0017
300	8	0.0728	0.0022
240	10	0.0724	0.0014
200	12	0.0730	0.0017
160	15	0.0729	0.0013
120	20	0.0728	0.0016
100	24	0.0730	0.0011
80	30	0.0732	0.0015
60	40	0.0734	0.0014
50	48	0.0732	0.0017
40	60	0.0741	0.0012
30	80	0.0737	0.0015

*Total data length mT = 2400 sec.

deviation S_m, and the sample standard deviation with no averaging, S_1, reduced by a factor $m^{-1/2}$. The latter assumes that S_1 is the standard deviation of the population so that $S_1 m^{-1/2}$ gives the theoretical deviation of the sample mean of the roll-frequency estimates themselves, the mean in this case being the roll-frequency estimate $\hat{f}_\varphi$ determined from an average of m spectra.

A logical question to ask at this point is whether the reduction so achieved results from the averaging or from the increased amount of data mT that entered into the determination of a single estimate of the roll frequency. To investigate this the total length mT of data was fixed while the sample length T and the number m of spectra averaged were varied. From Table 8 the deviation is seen to vary little, which suggests that the controlling parameter is the amount of data that enters into the determination of a single estimate of the roll frequency. The results of a series of such measurements for a variety of data lengths mT are shown in Fig. 13, where the mean deviation $\bar{S}_m$ is plotted as a function of the total data length mT. The equation fitted to the data, applicable over the range $30 \leqslant T$, is seen to be of the same form as that for the reduction in the deviation of the sample mean. It is necessary to restrict the range of T since for $T < 30$ sec there is insufficient resolution for the measurement accuracy desired.

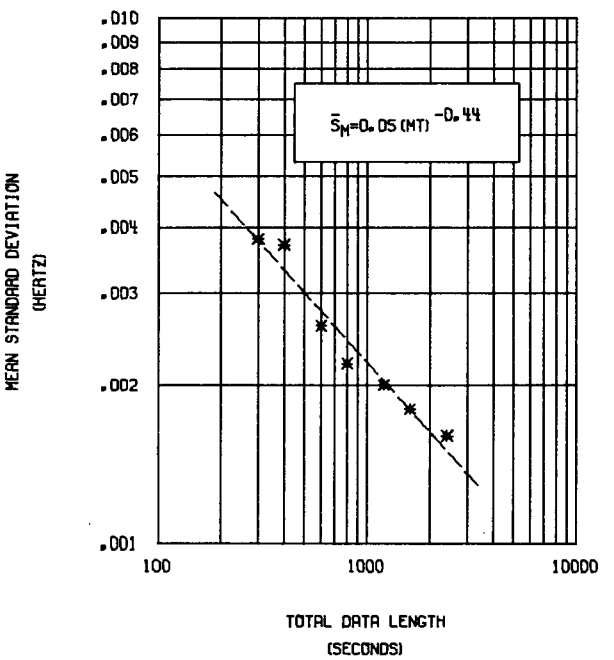

Fig. 13 — Mean standard deviation of roll-frequency estimates for different sample lengths vs total length of data per estimate

On examining Table 8 more closely one notices a global minimum in the deviation for a sample length T of 100 sec. In fact, this minimum was in evidence at other values of mT, which suggests that, given a length of data, the optimum processing requires that the

record be subdivided into 100-sec samples without regard to the number m of spectra to be averaged. The reason for this is to be found by examining the autocorrelation function for the roll history, Fig. 1. Immediately obvious is the almost total decorrelation for a lag of 100 sec. For a sample length less than this the samples would not be independent, in which case the reduction in the variance that results from averaging a given number of spectra would not be expected to be as great. Taking a sample length equal to the decorrelation time is in some respects equivalent to matched filtering or to enhancement of the signal-to-noise ratio by coherent integration.

The equivalence to matched filtering can be appreciated by considering that the decorrelation time is approximately the reciprocal of the resonant bandwidth. To choose a rectangular data window with a length equal to the decorrelation time is to choose a spectral window with a bandwidth comparable to the bandwidth of the resonant peak. Such a matching of the functions being cross correlated (the convolution of even functions) as a consequence of transforming should result in maximum response of the "filter" at the frequency of resonance. If some weighting other than rectangular were used, leading to spectral windows with larger bandwidths, the truncation length would have to increase to maintain bandwidth equality.

The equivalence to coherent integration can be understood by considering that, because of the coherence of the signal, signal energy builds up in the output of the filter while the noise energy, through destructive interference, remains at about the same level. As we include more and more cycles of the coherent signal, the peak in the spectrum corresponding to the center frequency of the oscillations grows higher and narrower. When the sample length exceeds the coherence length, the improvement ceases, and the single peak may split into multiple peaks, as seen in the closely spaced peaks in the spectrum of Fig. 14, obtained from 200 sec of data. The two peaks of almost equal amplitude may represent two frequency components present simultaneously or the frequencies of adjacent groups of oscillations. In the former case, a smaller sample length will result in less resolution—as shown in the spectrum of Fig. 15, obtained from 100 sec of data—thereby effectively averaging the two spectral lines and simultaneously increasing the number of spectra available for averaging. In the other case, where the two peaks represent the frequencies of adjacent groups of oscillations, halving the sample length could result in measuring each peak separately, with the result that both would be accounted for and twice as many spectra would be available for averaging.

It is interesting to note that the decorrelation time of 100 sec, which spans about seven cycles of the roll history, appears to correlate with the coherence length of the frequency component in the sea that is driving the ship in the roll plane. Measurements by Crombie et al. [41] of high-frequency groundwave backscatter from the sea indicate coherence lengths of 3.5 to 9.4 cycles for waves with a period equal to that of the ship's roll.

Since ship roll histories are signallike in character, spectral windows find use primarily in reducing errors in the measurement resulting from leakage through their sidelobes. An interesting problem arises in the spectral analysis of ship roll histories where we are interested in the frequency of a strong spectral line near $f = 0$. For small sample lengths, leakage from the negative-frequency image of the spectral peak can introduce significant error in estimating the frequency of the peak. Aspects of this problem are treated on pp. (35 - 38)

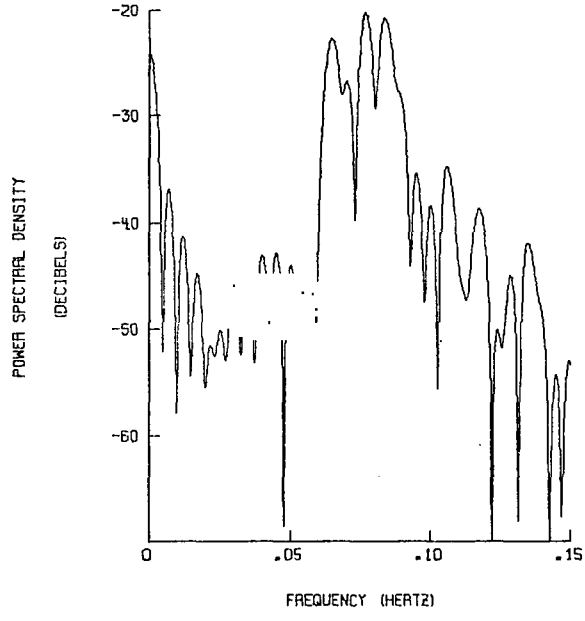

Fig. 14 — Power spectrum of the ship roll history of the USS *Providence*, February 16, 1972 (T = 200 sec)

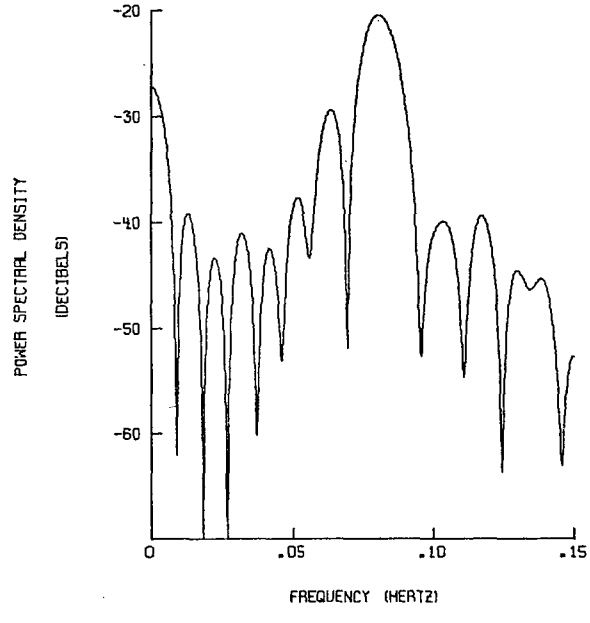

Fig. 15 — Power spectrum of the ship roll history of the USS *Providence*, February 16, 1972 (T = 100 sec)

and in Appendix B. The problem is minimized here since an optimum sample length equal to the decorrelation time of the roll record, chosen for other reasons, places the sample length in a regime (i.e., $T/T_0 > 6$, see Appendix B) where the error (Fig. A2 is less than 1%. For the smaller sample lengths in Table 8, however, the behavior depicted by Figs. A2 and A3 explains the source of some of the scatter (larger deviation) in the measurements since for those data the truncation length was fixed while the phase was allowed to vary randomly. This also explains why the deviation in Table 8 oscillates with sample length for the smaller sample lengths.

The last factor to be considered that affects the processing of the data is the method of averaging. Do we average normalized or unnormalized power spectra, contiguous or noncontiguous samples? There are reasons that suggest that each technique has merit. For example, we might suppose from an examination of a roll history that the largest oscillations are large because they are closer in frequency to the natural roll frequency we are endeavoring to measure, as suggested by Vossers [2] and Williams [8], and that such oscillations should receive greater weight in the averaging process. This will be the case if we average power spectra. On the other hand, if we average normalized power spectra (normalized to the total power in the spectrum), we give equal weight to each member of the ensemble over which the average is being taken. This is to be preferred if the amplitude of the oscillations is not a measure of their proximity to resonance. A comparison of the two methods of averaging is summarized in Table 9, where the sample standard deviation of the roll-frequency estimates from averaging normalized power spectra, S_m^1, is uniformly smaller than the sample standard deviation from averaging power spectra, S_m^2, and where $S_1 m^{-1/2}$ gives the theoretical reduction in the standard deviation that results from averaging roll-frequency estimates for a population having the standard deviation S_1. This suggests that the larger oscillations in the roll history do not signify proximity to resonance, as has been supposed, but have some other cause, such as coherence of the wave train driving the ship in roll.

Table 9 — Dependence of the Standard Deviation S_m of the Roll-Frequency Estimates on the Method of Averaging*

Number of Average Spectra	m	S_m^1 † (Hz)	S_m^2 ‡ (Hz)	$S_1 m^{-1/2}$ (Hz)
144	1	0.0071	0.0071	0.0071
72	2	0.0046	0.0047	0.0050
36	4	0.0033	0.0035	0.0036
18	8	0.0016	0.0021	0.0025
9	16	0.0012	0.0014	0.0018
6	24	0.0011	0.0015	0.0014

*Sample length T = 100 sec.
†Values for S_m^1 from averaging normalized power spectra.
‡Values for S_m^2 from averaging power spectra.

The consideration of averaging spectra computed from contiguous or noncontiguous segments of the roll history arose as the result of processing a 4-hr data tape from the USS *Providence* (CLG-6) recorded February 14, 1972. Conditions were such that the ship was driven well off resonance (at about 0.1000 Hz compared to a resonant frequency of 0.0730 Hz) for a period of about 20 min. Averaging spectra from contiguous segments of the roll history gave rise to some estimates of the roll frequency that were obviously too high. Moreover, the bad estimate persisted in spite of an increase in the number m of spectra averaged. The occurrence of such extended periods of rolling far from resonance has been noted.† To avoid obtaining a bad estimate of the roll frequency under such conditions we can separate our measurements by a time interval large enough to span the interval of bad data. This was done for the data in question, where the interval between measurements was $240/m$ min. For $m = 8$ the interval between measurements was 30 min, which means that one bad measurement was averaged with seven other measurements—a procedure that effectively discriminated against such an abnormality in the record.

The reason for the occurrence of such anomalies is not clear. The discussion of bias on pp. 35 - 38 relating to a shift in the frequency of the resonant peak resulting from the steepness of the wave-slope spectrum in the vicinity of resonance for low wind-speeds may be pertinent. If, for example, the local winds were below about 15 m/sec, giving rise to a wave-slope spectrum with a peak substantially higher in frequency than the roll-resonant frequency, and if the swell were unidirectional so that when heading into or away from the swell the ship were driven in roll by something approaching a Pierson-Moskowitz wave-slope spectrum [16] for low windspeeds, such a condition could obtain. Unfortunately, not enough information about the test conditions was available for making such a judgment. Two pieces of information are available, however, that support the plausibility of the argument above. Motion pictures of the sea taken in the operating area on the day for which the roll history is available show that the winds were very light, as indicated in Table 5, and show well-defined swell that may indeed have been unidirectional. A discrepancy between the times of observation in the table and the times recorded with the roll history would not allow correlation of the behavior with the angle between the ship's heading and the swell direction. A correlation between the occurrence of the high estimates of the roll frequency and the ship's heading did reveal, however, that the high estimates occurred on headings about 180 degrees apart, or on opposite sides of the box pattern being executed. Similar behavior was noted by Norrby and Engvall [13], who indicated that, when the vessel was sailing against the waves, the rolling and pitching were coupled, rendering the roll period small.

Sampling Distribution of Roll-Frequency Estimates

We have already seen (pp. 25 - 28) that the power-spectral estimates for white noise are distributed as chi-squared variates with two degrees of freedom and that averaging m such variates results in the average spectral estimates being distributed as chi-squared with $2m$ degrees of freedom. We saw also that extension of these results could be made to an arbitrary stochastic process providing that the sample length was large enough to make the width of the spectral window small compared to the structure of the power spectrum of the process or that the power spectrum of the process was smooth relative to the spectral window. These assumptions were made on pp. 30 - 35 in deriving for a known power

†A.E. Baitis, Naval Ship Research and Development Center, Bethesda, Md., private communcation, 1974.

spectrum the probability density function for the estimates of the resonant frequency given a finite number m of spectra from the ensemble so that the independent spectral estimates were distributed as chi squared with 2 m degrees of freedom. We saw there that the form of the probability distribution in the absence of bias (due to leakage through the sidelobes of the spectral window introduced by the finiteness of the sample length) was Gaussian. It was noted also that, although the probability density function for the estimate of the resonant frequency was dependent on the shape of the power spectrum of the process, only the spectrum in the vicinity of resonance contributed significantly to the probability. Hence, even for the case of two filters in tandem, one having as a transfer function the square root of the wave-slope spectrum for a Pierson-Moskowitz sea and the other having the transfer function for the ship in the roll plane, the probability density function for the estimates of the resonant frequency was Gaussian.

The result of processing one 4-hr roll history for the USS *Providence* are shown in the form of cummulative distribution functions plotted on normal probability paper. In Figs. 16 through 20 T is the sample length (seconds) from which a single sample spectrum was calculated and m is the number of sample spectra averaged to give a single estimate of the roll frequency plotted on these curves. Three methods of averaging the m spectra were used. In methods 1 and 2 normalized and unnormalized power spectra, respectively, were averaged; in both cases the spectra were computed from contiguous segments of the roll history. In method 7 normalized power spectra computed from non-contiguous segments of the roll history were averaged.

Figure 16 shows the cumulative distribution function for the global maxima from 144 individual power spectra, each computed from 100 sec of data. The sampling distribution in the absence of averaging is decidedly not Gaussian. The reduction in the variance and the tendency to normality with averaging are shown in Fig. 17, where normalized spectra from noncontiguous segments of the record were averaged. Figures 18 and 19 are included to show graphically the comparison between averaging unnormalized and normalized power spectra, in these two cases obtained from contiguous segments of the record. If the amplitude of the roll were a measure of the proximity to resonance, then we should have expected to see the smaller variance in Fig. 18, where the greater power in the larger oscillations near resonance would dominate in the averaging. However, this is seen not to be the case. Figure 20 is the sampling distribution for 12 hr of data with the measurements separated by 30 min.

It should be noted that the standard deviations are larger for the sampling distributions determined from actual data than those predicted on pp. 27 - 31. The relationship between the standard deviation for the fractional error ϵ and that for the estimated roll frequency $\hat{f}_\varphi$ can be shown to be

$$\sigma_{\hat{f}_\varphi}(m) = f_\varphi \sigma_\epsilon(m).$$

For a natural roll frequency f_φ of 0.0730 Hz and a standard deviation $\sigma_\epsilon(m)$ for the fractional error for $m = 8$ equal to 0.0095, the standard deviation $\sigma_{\hat{f}_\varphi}(m)$ for the roll-frequency estimate would be 0.0007 Hz. Figure 20 shows the standard deviation for $m = 8$ to be 0.0025 Hz.

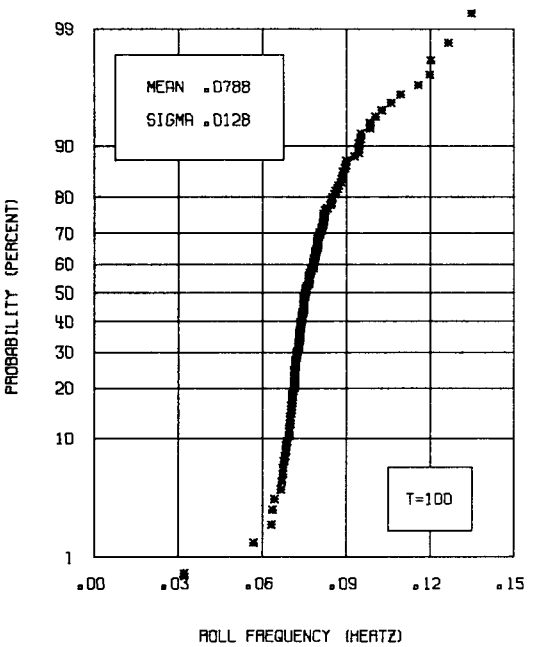

Fig. 16 — Cumulative distribution function of roll-frequency estimates, USS *Providence*, February 14, 1972 (m = 1)

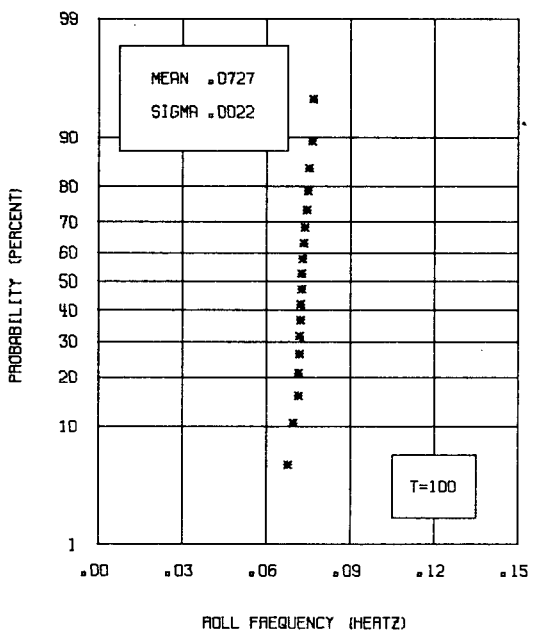

Fig. 17 — Cumulative distribution function of roll-frequency estimates, USS *Providence*, February 14, 1972 (method 7, m = 8)

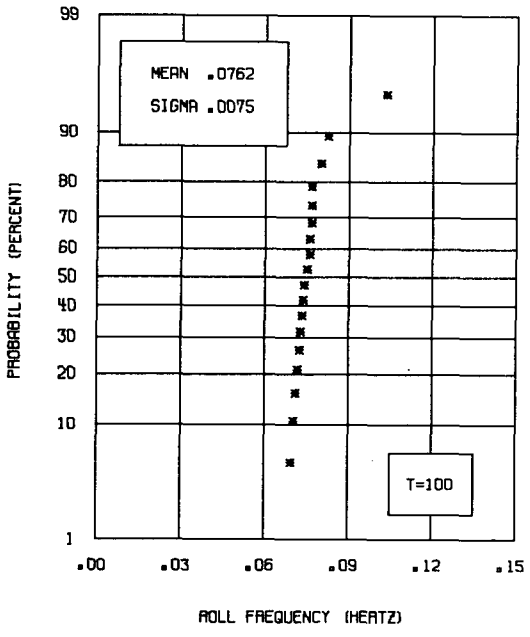

Fig. 18 — Cumulative distribution function of roll-frequency estimates, USS *Providence*, February 14, 1972 (method 2, m = 8)

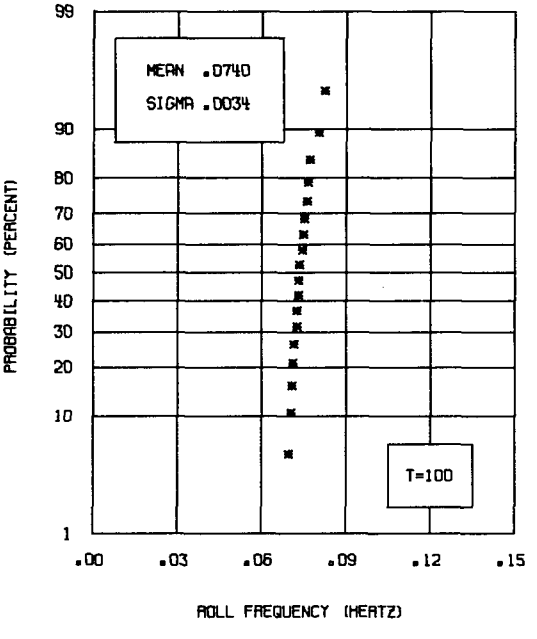

Fig. 19 — Cumulative distribution function of roll-frequency estimates, USS *Providence*, February 14, 1972 (method 1, m = 8)

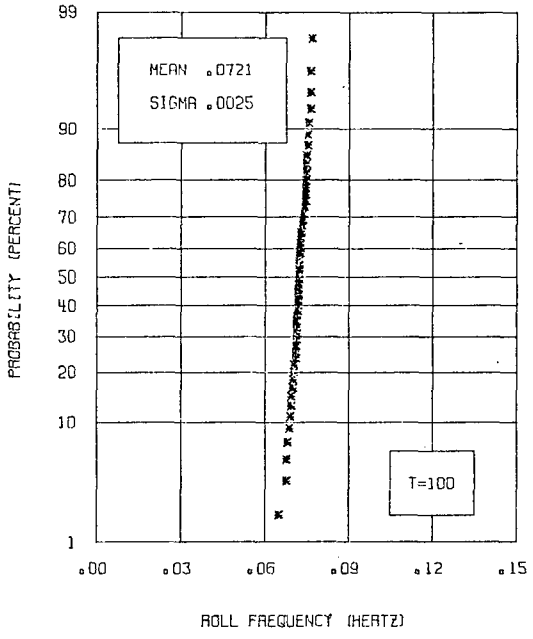

Fig. 20 — Cumulative distribution function of roll-frequency estimates, USS *Providence*, three reels (method 7, m = 8)

This discrepancy is not surprising since in our earlier discussion on pp. 27 - 31 we assumed a roll-damping coefficient of 0.032 and assumed that the spectrum of the driving force dia not alter the bandwidth of the resonant peak, whereas in practice neither of these conditions may have obtained. There are several possible causes of this variability: a differing doppler shift in the spectrum of the driving force for each of the eight courses on which the ship steamed; nonstationarity of the sea over the period during which the data was gathered; underestimation of the roll-damping coefficient, which would have the effect of reducing the bandwidth of the resonant peak in the power spectrum assumed in the derivation and therefore the variance of the roll-frequency estimates; and broadening of the resonant peak at sea resulting from the steepness in the spectrum of the driving force in the vicinity of resonance causing an increase in the variance of the sampling distribution.

Comparison of the estimates of the natural roll frequency in Fig. 20 with the value obtained from inclining experiments in still water shows a close correlation. The natural roll period from inclining experiments [42] is found to be 13 to 14 sec (frequency 0.0714 to 0.0769 Hz), whereas the mean of the estimates of the natural roll frequency in Fig. 20 is 0.0721 Hz; this shows that the results of measurements made in a confused sea are in good agreement with those made in still water. In both cases the spread in the values is comparable, but it appears that measurement of the natural roll frequency by spectral analysis of the roll history, as described in this study, has the potential for significantly improving the accuracy of such measurements.

The method that has been employed until now for ships of the U.S. Navy consists of sallying the ship by hauling up on one side of the ship at dockside with a crane in

synchronism with the expected natural roll frequency until the oscillations are built up to a measurable level. Several observers with stopwatches then time the decaying oscillations. Not only is measurement error significant with this method but the tests are often made while the ship is in the yard completing an overhaul and not in its normal operating condition. A test that could be made with the ship fully loaded and in operating condition at sea would offer distinct advantages. The test could be as simple as recording the roll history while the ship is at sea for later processing ashore. The equipment required would therefore be minimal. Since time is likely not to be urgent for such an application, the large amount of data that could be gathered and processed could lead to very accurate measurements. Processing of the same 12 hr of data for the USS *Providence* as shown in Fig. 20 but for m = 36 (averaging thirty-six 100-sec sample spectra spaced 20 min apart) so that each measurement represents 1 hr of data yields a mean value for the estimate of the natural roll frequency of 0.0725 Hz with a standard deviation of 0.0008 Hz.

Correlation of Roll Frequency With Ship Size

Figures 21 through 24 show the roll frequency for 13 ships plotted as a function of overall length, beam at the waterline, maximum navigational draft, and full-load displacement. To assess the degree of correlation with each of these parameters a least-squares regression line was fitted to the data and the rms error was computed.

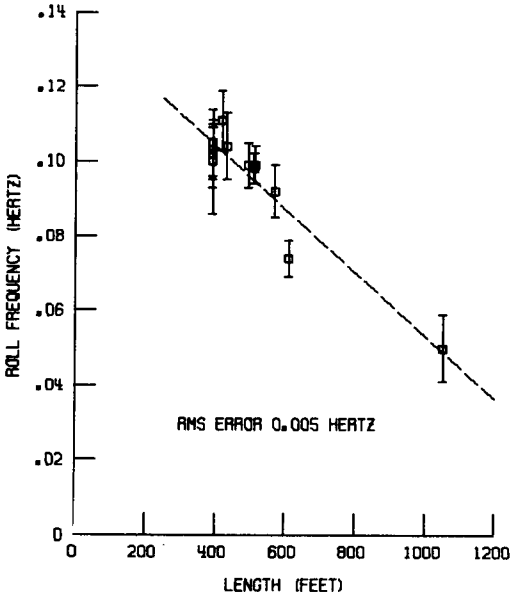

Fig. 21 — Correlation of roll frequency with ship length (1 ft = 0.3048 m)

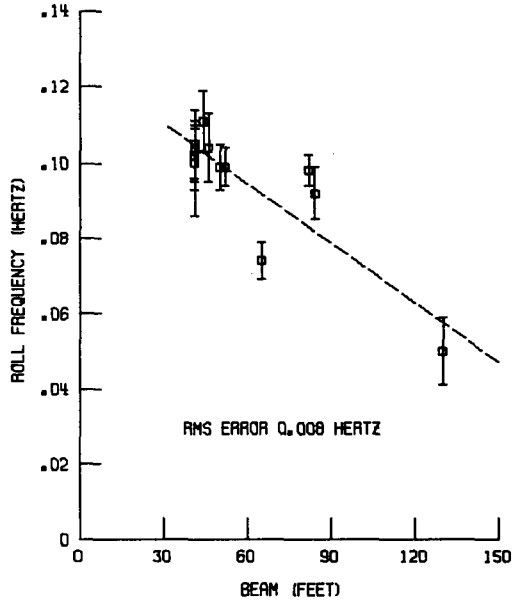

Fig. 22 — Correlation of roll frequency with ship beam (1 ft = 0.3048 *m*)

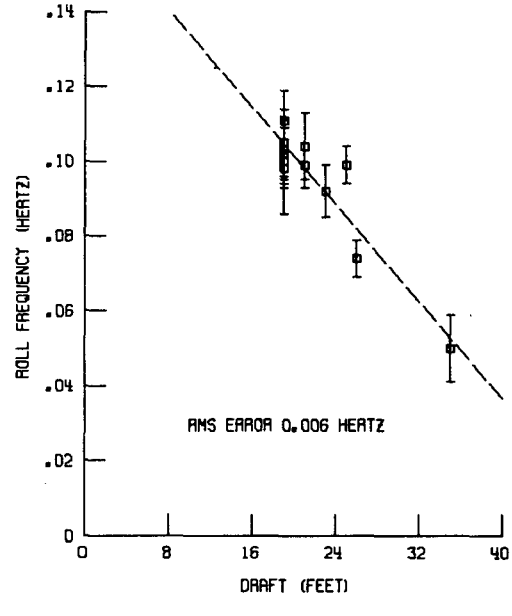

Fig. 23 — Correlation of roll frequency with ship draft (1 ft = 0.3048 *m*)

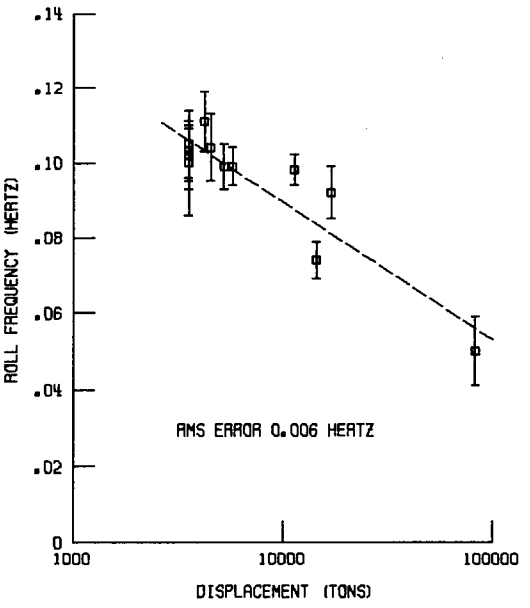

Fig. 24 — Correlation of roll frequency with ship displacement

The algorithm for selecting the roll frequency for each of the 13 ships made use of no *a priori* knowledge about the size of the vessel or its probable roll frequency but assumed only that the roll frequency lay in the band of frequencies from 0.0350 to 0.1250 Hz, which spans the range of roll frequencies from large aircraft carriers to small destroyers.

Interestingly, the best correlation of the natural roll frequency is with the length of the vessel, and not with the beam or draft, which we would suppose to be more strongly correlated with the radius of gyration, the metacentric height, and the righting arm. The dependence of the natural roll frequency on these parameters can be seen by considering the case of unresisted roll in still water. For these conditions Eq. (1) reduces to the following simple form:

$$\frac{d^2\varphi}{dt^2} + \omega_r^2\varphi = 0. \tag{66}$$

From first principles, if it is assumed that the axis of roll passes through the center of gravity G, the equation of motion may be written

$$I\frac{d^2\varphi}{dt^2} + M = 0 \tag{67}$$

where I is the mass moment of inertia about the roll axis through the center of gravity and M is the righting moment. The moment of inertia may be written

$$I = \frac{\Delta k^2}{g} \tag{68}$$

where Δ is the displacement of the vessel, k is the radius of gyration of the mass of the ship about the roll axis, and g is the acceleration due to gravity. From Fig. B3 in Appendix B, we can see that for small angles of inclination the righting moment may be written

$$\begin{aligned} M &= \Delta\overline{GZ} \\ &= \Delta\overline{GM}\sin\varphi \\ &= \Delta\overline{GM}\,\varphi \end{aligned} \tag{69}$$

where $\overline{GZ}$ is the righting arm and $\overline{GM}$ is the metacentric height. Substitution of Eqs. (68) and (69) into Eq. (67) gives

$$\frac{d^2\varphi}{dt^2} + g\frac{\overline{GM}}{k^2}\varphi = 0. \tag{70}$$

A comparison of Eqs. (66) and (70) shows that the radian frequency for unresisted roll in still water is given in terms of the parameters of static stability as

$$\omega_r^2 = \frac{g\,\overline{GM}}{k^2}.$$

Making use of the relation $\omega_r = 2\pi f_r$ and the expression for the natural roll frequency in terms of the frequency of unresisted roll in still water, Eq. (3), we obtain

$$f_\varphi = \frac{(g\,\overline{GM})^{1/2}}{2\pi k}\,(1-\kappa^2)^{1/2}. \tag{71}$$

The close correlation between the natural roll frequency and the length, which appears nowhere in the above equations, is probably attributable to the existence of an "aspect" ratio among the size parameters of length, beam, draft, and displacement. A similar correlation for the still-water roll period for British warships was noted by Williams [8]. Assuming similarity of form (geometrical) and weight distribution, he gave the empirical relation as

$$T_\varphi \propto \ell^{1/2} \tag{72}$$

where T_φ is the natural period of roll and ℓ is any linear dimension (e.g., length, beam, or draft). The symbol $\propto$ indicates proportionality. Correlation with displacement Δ was given as

$$T_\varphi \propto \Delta^{1/6}. \tag{73}$$

It is interesting to note that the correlation due to Williams [8] is not linear with linear dimension; the natural roll period varies as the square root of the linear dimension. The correlations shown in Figs. 21 through 24 suffer from a lack of data for larger ships, the USS *John F. Kennedy* being well removed in size from all the others for which data is plotted. If data for ships intermediate in size between the USS *Providence* and the USS *John F. Kennedy* were plotted, they might be expected to fall below the least-squares regression

line in Fig. 21, in which case Williams' [8] result would appear to apply. It is also interesting to observe that the data for the USS *Thomaston* (LSD-28) and the USS *Coronado* (LPD-11) amphibious ships differing in geometrical form from the others, which are ships of the line, fall close to the regression line in Figs. 21 and 23; this indicates close correlation of their natural roll periods with length and draft. Figures 22 and 24 indicate that the data for these same two ships may well be biasing the correlation in favor of a linear relationship since these ships fall in the middle of the range of beam and displacement and the data lies above the regression line.

CONCLUSIONS AND RECOMMENDATIONS

Conclusions

The optimum processing of a finite length of roll history (optimum in the sense of minimum variance in the estimate of the natural roll frequency) consists of (a) partitioning the record into m segments T seconds long, T being the decorrelation time of the roll history; (b) weighting the data with a rectangular data window for optimum bandwidth of the spectral window; (c) adding zeros to each segment of the weighted data before transforming to achieve the desired fineness in frequency; (d) computing the squared modulus of the Fourier transform of the weighted data with zeros added; (e) normalizing the resulting spectrum to unity total power; (f) averaging the m normalized sample power spectra to obtain a smoothed estimate of the roll spectrum; (g) determining the frequency of the global maximum of the roll spectrum; (h) correcting this estimate of the resonant frequency for the bias introduced by the steepness of the driving-force spectrum in the vicinity of resonance if this information is available; and (i) computing the estimate of the natural roll frequency from a deterministic relation involving the estimated resonant frequency and the coefficient of roll damping if the latter is large enough to necessitate such a correction.

Where the amount of data is not so limited and there is the opportunity for designing the experiment, the optimum procedure is to average sample spectra computed from noncontiguous portions of the roll history separated by 30 min or more and representing a diversity of ship headings.

Although it is true that a ship, which is a narrowband resonant system in the roll plane, is not likely to be driven to large angles of roll at frequencies far from resonance, it is not true that the size of the oscillations is necessarily a measure of proximity to resonance. This was discovered by a comparison of averaging techniques. It was argued that if large-amplitude rolling obtained by virtue of proximity to resonance, then the heavier weighting given to spectra from such portions of the record by averaging unnormalized power spectra would lead to a smaller variance in the measurement. This was not the case, but averaging normalized power spectra (thereby giving equal weight to each portion of the roll record regardless of the amplitude of the oscillations) led to the smaller variance.

The probability distribution for the estimates of the natural roll frequency determined by the optimum processing scheme described above was derived and found to be Gaussian. This was confirmed by measurements of 12 hr of roll history from the USS *Providence.*

The Pierson-Moskowitz spectrum [16], as a model for the sea, indicates accurate measurement of the natural roll frequency for windspeeds above 20 m/sec for which the resonant frequency is on the relatively flat portion of the spectrum. For lower windspeeds the Pierson-Moskowitz spectrum is inadequate as a model since there is insufficient energy in this spectrum in the vicinity of roll resonance. In practice, the presence of swell resulting from stronger wind systems over other portions of the ocean overcomes this deficiency so that a ship manages to roll most of the time.

Correlation of the natural roll frequency with ship-size parameters (length in particular) for American warships suggests that measurements of the natural roll frequency, if they could be made from radar-cross-section histories of ship targets, be used to classify radar targets in a remote-sensing system.

Recommendations for Future Research

In the classic work in modern times on ship motions at sea, St. Denis and Pierson [6] made the powerful assumption of linearity that provided new impetus to the study of the interaction between ship and sea. The validity of the linearity assumption was confirmed by Lalangas [19] for the regimes of small roll angle or high ship speed. For most of the ships whose behavior is discussed in this report the roll angles were small, so that the assumption of linearity could be made. The assumption of uncoupled motions, also made by St. Denis and Pierson, neglected the coupling of pitch, heave, and roll treated by Nayfeh et al. [43] and the coupling of the lateral motions of roll, sway, and yaw treated by Tasai [44]. With the development of techniques to handle nonlinear, coupled motions, the analysis reported here might be extended to such cases.

The point was made on pp. 35 - 36 that for low windspeeds the steepness in the spectrum of the driving force in the vicinity of resonance (based on a Pierson-Moskowitz model [16] for a fully developed sea) was so large as to completely obliterate the resonant peak in the roll spectrum. On the other hand, as noted on pp. 46 - 47, the USS *Providence* (CLG-6) was excited into roll resonance although the local windspeed was only about 5 m/sec. The explanation, as as given on pp. 36 - 38, was that the Pierson-Moskowitz spectrum is an equilibrium condition that rarely obtains except in certain regions such as the tropics, where the trade winds have both the fetch and duration to cause the sea to attain equilibrium. Moreover, this model for the sea does not take into account the presence of swell propagating into the area from distant storms. Kinsman [37] indicates the frequency of the swell to be below 0.1 Hz, which is precisely the region of roll resonance for most large ships.

Clearly, what is needed is a statistical description of the sea in terms of probability distributions for the spectral estimates where the variability reflects the variation in the sea with such parameters as windspeed, time of day, and season of the year—and such other parameters as may be correlated with the general meteorological conditions that affect the spectrum. According to L. Moskowitz,† such a description has not even been attempted, although wave-height records covering the period from 1952 to the present are available from the Institute of Ocean Studies (formerly the National Institute of Oceanography) for English weather ships located at stations India (59°N, 19°W) and Juliet (52.5°N, 20°W)

† Private communication to the author, 1975.

in the North Atlantic Ocean. It might prove interesting to derive empirically the means and standard deviations of the spectral estimates for the wave-height records from these two weather stations and to attempt to identify trends (e.g., daily, weekly, monthly, quarterly, and yearly).

The results of such a study might indicate how the estimate of the natural roll frequency might be corrected for bias due to the steepness in the spectrum of the driving force in the vicinity of resonance for cases of low windspeed.

An assumption made on pp. 15 - 16 to render the mathematics more tractable was that the motion of the ship through the sea would not alter appreciably the spectrum of the driving force. This assumption obviated the need for a rather tedious transformation to an "encounter" spectrum. Neither this nor the assumption of a frequency-independent spreading function also made on p. 14 should affect the smoothness of the spectrum driving the ship in roll. A more rigorous rendering of the mathematics in these two cases would be useful in confirming the accuracy of the simpler treatment considered here.

Another area in which research might be fruitful is an extension of the spectral analysis techniques, applied here to ship roll histories, to ship radar-cross-section histories since the correlation of the natural roll frequency with ship-size parameters suggests that the natural roll frequency might serve to classify a ship target as to size. A modest effort could be made by a computer simulation of the radar-cross-section history using as inputs to the program the appropriate radar-cross-section patterns for the ship and actual yaw, roll, and pitch histories. Application of the technique described above to the simulated radar-cross-section histories and simultaneously to the roll histories should provide a measure of how successfully the natural roll frequency can be extracted from radar data.

ACKNOWLEDGMENTS

The author extends his appreciation to Donald F. Hemenway, who first suggested the study of ship roll frequency; to Robert E. Ellis, Norman W. Guinard, and Edward N. Carey, who, as branch heads, provided the opportunity and encouragement to pursue this work; and to the Naval Research Laboratory for its exceptional facilities. Special mention should be made of A. Erich Baitis of the Naval Ship Research and Development Center and of Michael B. Laing and Denzil Stilwell of the Naval Research Laboratory, whose discussions with the author on ship dynamics, spectral analysis, and ocean wave spectra, respectively, helped to clarify important points of the theory. The author also wishes to thank Pasquale DeLeonibus of the Naval Oceanographic Office, who provided the wave-height records from the Argus Island. Mention should be made also of Mrs. Stella D. Scates, who typed the several drafts of the manuscript, and to Mrs. Betty J. McDonald, who assisted.

REFERENCES

1. R. Norrby, "The Stability of Coastal Vessels," Trans. R.I.N.A. **104**, 517 (1962).

2. G. Vossers, Jr., *Resistance, Propulsion, and Steering of Ships*, Vol. C, *Behavior of Ships in Waves*, H. Stam, N.V., Haarlem, The Netherlands, 1962.

3. W. Froude, "On the Rolling of Ships," Trans. I.N.A. 3, 180 (1861).

4. A. Kriloff, "A General Theory of the Oscillations of a Ship on Waves," Trans. I.N.A. 40, 135 (1898).

5. G. Weinblum and M. St. Denis, "On the Motions of Ships at Sea," Trans. S.N.A.M.E. 58, 184 (1950).

6. M. St. Denis and W.J. Pierson, Jr., "On the Motions of Ships in Confused Seas," Trans. S.N.A.M.E. 61, 280 (1953).

7. N. Barber, "Simultaneous Frequency Analyses of Waves and Ship Movement," ARL Report No. 103.40/R.1/W, 1945.

8. A.J. Williams, "An Investigation into the Motions of Ships at Sea," Trans. I.N.A. 95, 70 (1953).

9. D.E. Cartwright and L.J. Rydill, "The Rolling and Pitching of a Ship at Sea, a Direct Comparison Between Calculated and Recorded Motions of a Ship in Sea Waves," Trans. I.N.A. 99, 100 (1957).

10. W. Marks, "The Application of Spectral Analysis and Statistics to Seakeeping," Technical and Research Bulletin No. 1-24, the Society of Naval Architects and Marine Engineers, 1963.

11. A.E. Baitis and R. Wermter, "A Summary of Oblique Sea Experiments Conducted at the Naval Research and Development Center," Report of the Seakeeping Committee, Appendix VIII, in 13*th International Towing Tank Conference* 1972, Berlin/Hamburg, September 4-14, 1972.

12. W. Langmaack, "Haufigkeitsverteilung der Schwingungsperioden und Amplituden eines Schiffes in Seegand," Werft-Reederei-Hafen 13, 204 (1941).

13. R. Norrby and L.O. Engvall, "Statistical Analysis of the Rolling Motion of Three Coasters," Eur. Shipbuilding, No. 4, 76 (1964).

14. S. Tamiya and S. Motora, *Advances in Research on Stability and Rolling of Ships*, Society of Naval Architects (Japan), 60th Anniversary Series, 1960, p. 6.

15. D. Stilwell, Jr., and R.O. Pilon, "Directional Spectra of Surface Waves from Photographs," J. Geophys. Res. 79, 1277 (1974).

16. W.J. Pierson and L. Moskowitz, "A Proposed Spectral Form for Fully Developed Wind Seas Based on the Similarity Theory of S.A. Kitaigorodskii," J. Geophys. Res. 69, 5181 (1964).

17. J.P. Comstock, editor, *Principles of Naval Architecture*, the Society of Naval Architects and Marine Engineers, New York, 1967.

18. V.K. Korvin-Kroukovsky, "Investigations of Ship Motion in Regular Waves," Trans. S.N.A.M.E. 63, 386 (1955).

19. P.A. Lalangas, "Application of Linear Superposition Techniques to the Roll Response of a Ship Model in Irregular Beam Seas," Davidson Laboratory, Stevens Institute of Technology, Report 983, March 1964.

20. N. Wiener, "Generalized Harmonic Anlaysis," Acta Math. 55, 117 (1930).

21. A. Khintchine, "Korrelationstheorie der stationaren stochastischen Prozesse," Math. Ann. 109, 604 (1934).

22. M.S. Longuet-Higgins, D.E. Cartwright, and N.D. Smith, "Observations of the Directional Spectrum of Sea Waves Using the Motions of a Floating Buoy," in *Ocean Wave Spectra*, Proceedings of a Conference, Easton, Md., May 1-4, 1961, pp. 111-136; Prentice-Hall, Englewood Cliffs, N.J., 1963.

23. C. Cox and W. Munk, "Statistics of the Sea Surface Derived from Sun Glitter," J. Marine Res. 13, 198 (1954).

24. C. Cox and W. Munk, "Measurement of the Roughness of the Sea Surface from Photographs of the Sun's Glitter," J. Opt. Soc. Amer. 44, 838 (1954).

25. S.A. Kitaigorodskii, *The Physics of Air-Sea Interaction*, Israel Program for Scientific Translations, Jerusalem, 1973.

26. W.J. Pierson, Jr., G. Neumann, and R.W. James, "Practical Methods for Observing and Forecasting Ocean Waves by Means of Wave Spectra and Statistics," H.O. Publication 603, U.S. Navy Hydrographic Office, 1955.

27. J. Darbyshire, "A Further Investigation of Wind-Generated Waves," Deut. Hydrograph. Z., 12, 1-13 (1959).

28. D.E. Cartwright, "The Use of Directional Spectra in Studying the Output of a Wave Recorder on a Moving Ship," in *Ocean Wave Spectra*, Proceedings of a Conference, Easton, Md., May 1-4, 1961; Prentice-Hall, Englewood Cliffs, N.J., 1963.

29. R.B. Blackman and J.W. Tukey, *The Measurement of Power Spectra*, Dover, New York, 1959.

30. G.M. Jenkins and D.G. Watts, *Spectral Analysis and Its Applications*, Holden-Day, Inc., San Francisco, 1968.

31. A. Schuster, "On the Investigation of Hidden Periodicities with Application to a Supposed 26 Day Period of Meteorological Phenomena," Terrestrial Magnetism 3, 13 (1898).

32. E. Slutsky, "The Summation of Random Causes as the Source of Cyclic Processes," Econometrika 5, 105 (1937).

33. P.J. Daniell, "Discussion on Symposium on Autocorrelation in Time Series," J. Roy. Stat. Soc. B8, 88 (1946).

34. D.G. Kendall, "Oscillatory Time Series," Nature 161, 187 (1948).

35. M.S. Bartlett, "Smoothing Periodograms from Time Series with Continuous Spectra," Nature 161, 686 (1948).

36. *CRC Handbook of Tables for Mathematics*, 4th ed., Chemical Rubber Company, Cleveland, 1964, p. 584.

37. B. Kinsman, *Wind Waves*, Prentice-Hall, Englewood Cliffs, N.J., 1965.

38. B.E. Kremer, G.W. Hermann, and F. Sollner, Jr., "Ship's Motion Recording System," NRL Memorandum Report 2489, August 1972.

39. John E. Moore, editor, *Jane's Fighting Ships*, 1975, Jane's Yearbooks, London, England.

40. B.M. Oliver, J.R. Pierce, and C.E. Shannon, "The Philosophy of PCM," Proc. I.R.E. 36, 1324 (1948).

41. D.D. Crombie, J.M. Watts, and W.M. Beery, "Spectral Characteristics of HF Ground Wave Signals Backscattered from the Sea," in *AGARD Conference Proceedings No. 77 on Electromagnetics of the Sea, Paris, June* 22-25.

42. "The Inclining Experiment for USS *Providence* (CLG 6)," Naval Ship Engineering Center, Hyattsville, Md., July 1970.

43. A.H. Nayfeh, D.T. Mook, and L.R. Marshall, "Nonlinear Coupling of Pitch and Roll Modes in Ship Motions," J. Hydronaut. 7, 145 (1973).

44. F. Tasai, "Ship Motions in Beam Seas," Report of the Research Institute for Applied Mechanics, Kyushu Universary, Vol. XIII, No. 45, 1965.

BIBLIOGRAPHY

Barber, N.F., "Finding the Direction of Travel of Sea Waves," Nature 174, 1048 (1954).

Bartlett, M.S., "Periodogram Analysis and Continuous Spectra," Biometrika 37, 1 (1950).

Bingham, C., Godfrey, M.D., and Tukey, J.W., "Modern Techniques of Power Spectrum Estimation," IEEE Trans. AU-15, 56 (1967).

Bracewell, R.N., *The Fourier Transform and Its Applications*, McGraw-Hill, New York, 1965.

Brigham, E.O., and Morrow, R.E., "The Fast Fourier Transform," IEEE Spectrum 4 (12), 63 (Dec. 1967).

Cooley, J.W., and Tukey, J.W., "An Algorithm for the Machine Calculation of Complex Fourier Series," Math. Comp. 19, 297 (1965).

Jenkins, G.M., "General Considerations in the Analysis of Spectra," Technometrics 3, 133 (1961).

Longuet-Higgins, M.S., "Measurement of Sea Conditions by the Motions of a Floating Buoy. Detection of Predominant Groups of Swell," Admiralty Research Laboratory Report 130.40/N5, 1946.

Moskowitz, L., "Estimates of the Power Spectrums for Fully Developed Seas for Winds Speeds of 20 to 40 Knots," J. Geophys. Res. 69, 5161 (1964).

Parzen, E., "Mathematical Considerations in the Estimation of Spectra," Technometrics 3, 167 (1961).

Parzen, E., "An Approach to Empirical Time Series Analysis," J. Res. Natl. Bur. Stnd. 68D, 937 (1964).

Pierson, W.J., "The Directional Spectrum of a Wind Generated Sea as Determined from Data Obtained by the Stereo Wave Observation Project," New York Univ. Meteorol. Papers, 2 (June 1960).

Stilwell, D., Jr., "Directional Energy Spectra of the Sea from Photographs," J. Geophys, Res. 74, 1974 (1969).

Tasai, F., "On the Sway, Yaw and Roll Motions of a Ship in Short Crested Waves," Report of the Research Institute for Applied Mechanics, Kyushu University, Vol. XIX, No. 62, 1971.

Welch, P.D., "The Use of Fast Fourier Transform for the Estimation of Power Spectra: A Method Based on Time Averaging Over Short, Modified Periodograms," IEEE Trans. AU-15, 70 (1967).

Yamanouchi, Y., "On the Analysis of the Ship Oscillations Among Waves—Part I," J. Soc. Naval Architects (Japan), 109 (1961).

Yamanouchi, Y., "Analysis of Irregular Wave Tests from Multiple Runs," Appendix III, Report of Seakeeping Committee, 13th International Towing Tank Conference, Berlin/ Hamburg, September 4-14, 1972.

Appendix A

ERROR IN ESTIMATING THE FREQUENCY OF A TRUNCATED SINUSOID

The problem of determining the frequency of a severely truncated sinusoid occurs quite often in the case of geophysical phenomena where the periods may be so long as to preclude observation of a number of cycles. The effect on the Fourier transform of severely truncating a sinusoid is to shift the frequency of the spectral maximum, an effect observed by Toman.† The explanation of this effect was provided by Jackson‡ and is reviewed here to help explain an oscillation in the variance of the roll-frequency estimator for short sample lengths.

The behavior of the error can be understood by considering the truncated sinusoid shown in Fig. A1a, where T_0 is the period of the sinusoid, τ is the delay from the start of the sinusoid to the first positive peak, and T is the truncation length of the sinusoid. The function $s(t)$ can be written

$$s(t) = \text{rect}\left[\frac{t - (T/2)}{T}\right] \cos\left(\frac{2\pi}{T_0} t + \varphi\right) \tag{A1}$$

where the phase angle $\varphi = 2\pi\tau/T_0$ and where rect $(t) = 1$ for $|t| < 1/2$ and is zero otherwise. By Fourier transformation we obtain the spectrum

$$S(\epsilon,\alpha,\varphi) = \frac{T_0}{2}\,\alpha\, e^{-i\pi(1+\epsilon)\alpha}\left[\text{sinc}(2+\epsilon)\alpha e^{-i(\pi\alpha+\varphi)} + \text{sinc}\,\alpha\epsilon e^{i(\pi\alpha+\varphi)}\right] \tag{A2}$$

where $\alpha = T/T_0$, $\epsilon = (f - f_0)/f_0$, and $f_0 = 1/T_0$. The sinc function is given by $\text{sinc}(x) = (\sin \pi x)/\pi x$. The notation for the spectrum $S(\epsilon,\alpha,\varphi)$ differs here from that used in the body of the dissertation, the meaning here being that the spectrum is a function of all three parameters shown.

Figure A1b, a plot of the magnitude of the spectrum for $\alpha = 2$ and $\varphi = 0$, shows the sinc-function spectral window replicated at f_0. It can readily be appreciated that adding the sidelobe from the spectral window centered at f_0 to the mainlobe at $-f_0$ will result in a shift in the location of the resulting peak where the slope of the sidelobe at $-f_0$ is not zero. A similar argument holds of course for the peak at f_0.

With the formulation of Eq. (A2) we can plot the fractional error ϵ in the position of the peak of the spectrum as the phase φ and the normalized truncation length α are varied. Figures A2 and A3 show this dependence.

†K. Toman, "The Spectral Shift of Truncated Sinusoids," J. Geophys. Res. 70, 1749 (1965).
‡P.L. Jackson, "Truncation and Phase Relationships of Sinusoids," J. Geophys. Res. 72, 1400 (1967).

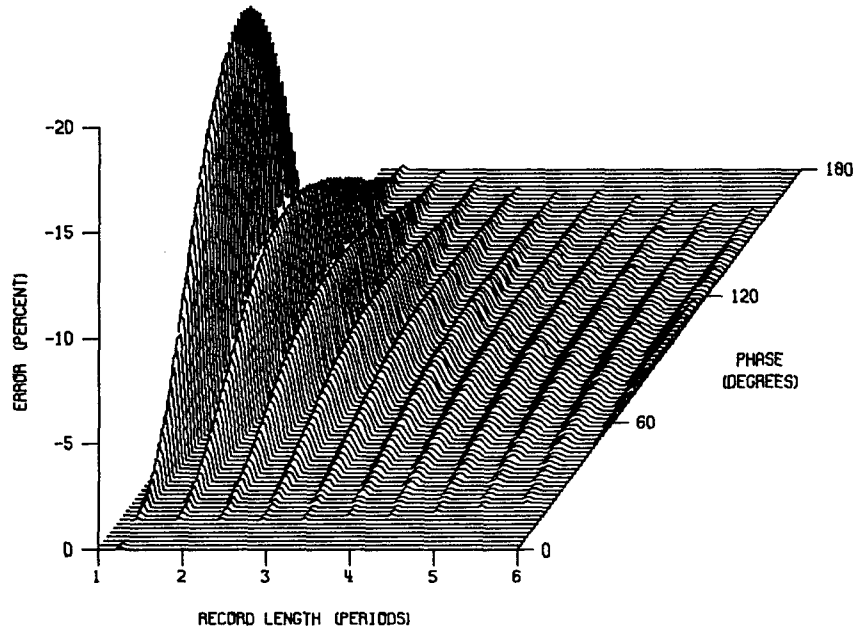

Fig. A3— Negative error in estimate of the frequency of a truncated sinusoid (mean retained)

could be reduced by choosing a spectral window with lower sidelobes. If the smaller bandwidth of the sinc-function spectral window cannot be compromised, it might then be advisable to choose, as nearly as one can, the phase and truncation length so as to minimize the error, for example,

$$\varphi = 0,$$

$$\alpha = 1.25 + \frac{n}{2}, \quad n = 1,2,3,\ldots,$$

although the algorithm for such a computation would be more complex. Fourth, since the error in this very simple model (i.e., a process spectrum consisting of a single spectral line and its image at negative frequency) arises from leakage due to the negative-frequency image, we could avoid the problem altogether by utilizing the analytic signal of Gabor.*

Since it is customary in spectral analysis to remove the mean from a sample of data before obtaining the spectrum, it would be of interest to know the effect on the error discussed above of removing the mean value of the sample before transforming. Removal of the sample mean leads to the spectrum

$$S'(\epsilon,\alpha,\varphi) = S(\epsilon,\alpha,\varphi) - \bar{s}T_0\alpha \operatorname{sinc}(1+\epsilon)\alpha e^{-i\pi(1+\epsilon)\alpha} \tag{A3}$$

*D. Gabor, "Theory of Communications," J. IEE (London) 93 (3), 429-457 (1946).

where the prime on the spectrum indicates that the mean has been removed and $\bar{s}$ is the mean of the truncated sinusoid, given by

$$\bar{s} = \frac{1}{2\pi\alpha}\left[\sin(2\pi\alpha + \varphi) - \sin\varphi\right]. \tag{A4}$$

The fractional error in this case is shown plotted in Figs. A4 and A5.

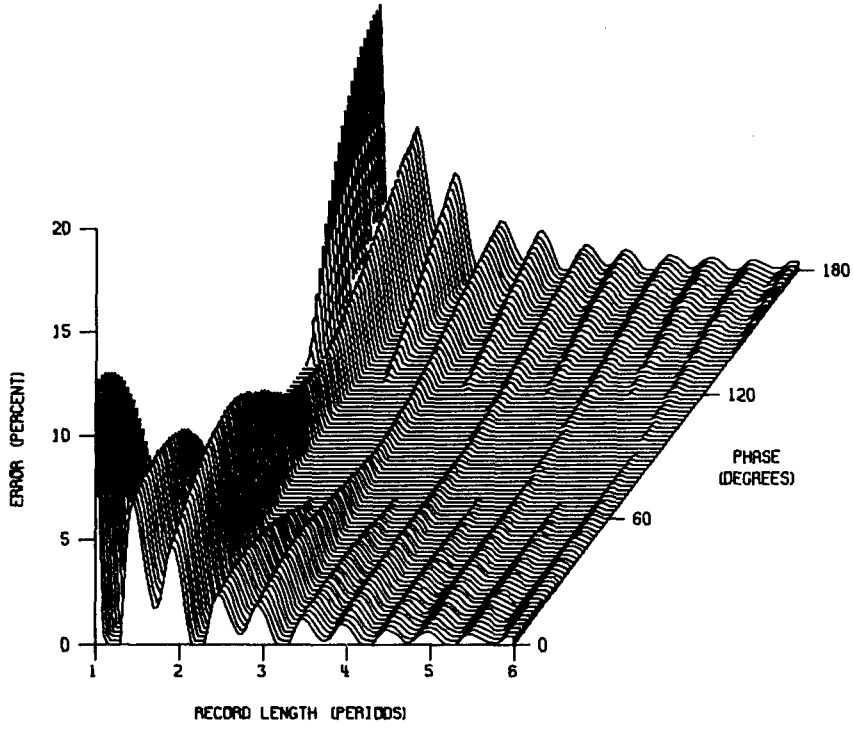

Fig. A4 — Positive error in estimate of the frequency of a truncated sinusoid (mean removed)

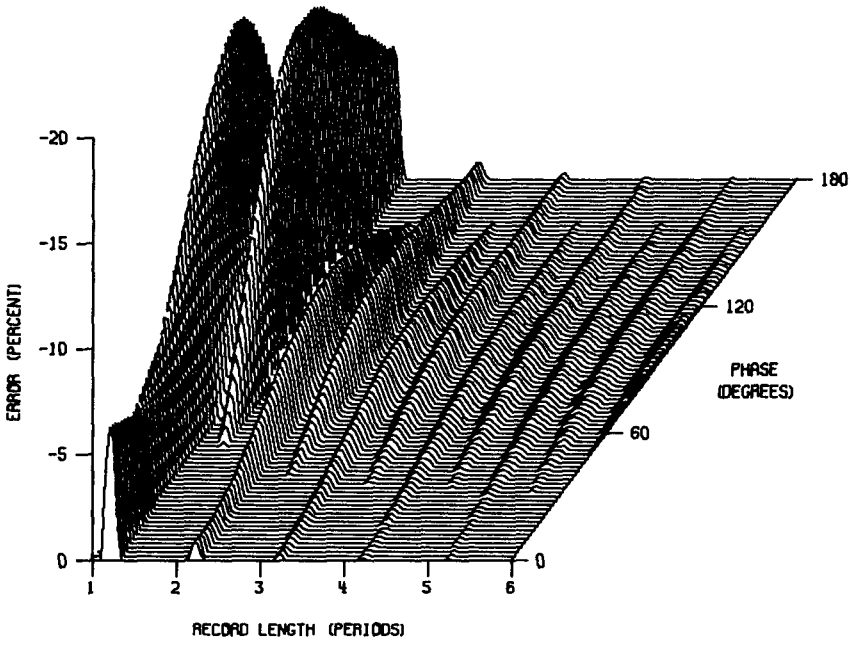

Fig. A5 — Negative error in estimate of the frequency of a truncated sinusoid (mean removed)

Appendix B

DEFINITION OF TERMS RELEVANT TO SHIP STABILITY

Naval Architecture

The motion of a ship in a seaway is characterized by six degrees of freedom: three translational (surge, sway, and heave) and three rotational (roll, pitch, and yaw). The relationship between the various component motions is shown in Fig. B1. Roll is the oscillatory motion of the ship in the sea, whereas heel is a temporary transverse inclination resulting from a high-speed turn or the influence of a strong wind. List is a more or less permanent condition of transverse inclination, such as might arise from uneven loading. Synchronous rolling, or the condition of synchronism, obtains when the apparent frequency of the swell (i.e., the frequency of that component normal to the roll axis) is very near the natural roll, or resonant, frequency of the ship. Resisted or unresisted rolling refers to the presence or absence of damping. Bilge keels are added to increase roll damping. They are longitudinal finlike structures protruding from the turn-of-the-bilge, or the point of maximum curvature of the underwater portion of the hull.

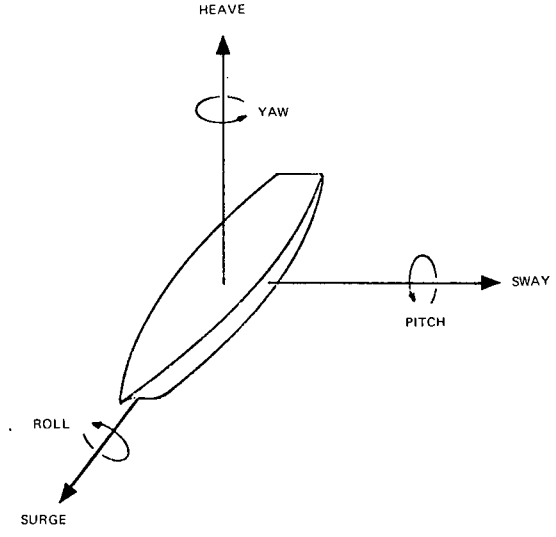

Fig. B1 — Relationship among the components of ship motion

Figure B2 shows the midship section, a plane normal to the longitudinal centerline plane and waterlines, the waterlines being planes (or their intersection with the hull) parallel to the base plane at the top of the flat keel. Shown in the figure are several angles of heel. For each angle of heel, or inclination, the shape of the displaced volume is different. The geometric center of the displaced volume is the center of buoyancy *B* through which the hydrostatic pressure on the immersed surface (equal to the weight of water

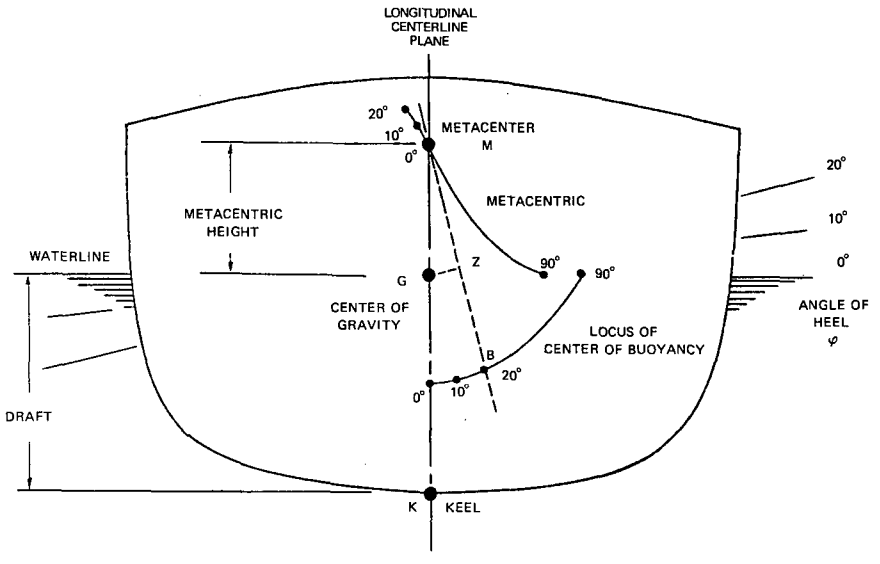

Fig. B2 — Transverse section showing parameters of static stability

displaced) acts vertically upward. The successive positions of the center of buoyancy for different angles of inclination describe a curve known as the locus of the center of buoyancy. For each point of this curve a center of curvature, or metacenter m, may be found. The locus of these metacenters is called the metacentric. For small angles of inclination, usually less than about 10 degrees, there is little change in the position of these centers of curvature. Hence, for small angles of inclination, these centers are assumed to be fixed in a position M called the metacenter.

Oceanography

The term "sea," as used by oceanographers, refers to waves generated or sustained by winds within their fetch, or distance over which the wind is interacting with the sea, whereas "swell" refers to waves that have traveled out of the area in which they were generated. Beam seas are wind-generated waves whose direction is normal to the roll axis, whereas a confused sea is a rough sea (waves 1.5 to 2.5 m (5 to 8 ft) high produced by winds of about 8 m/sec) where the direction and period of the sea and/or swell are indeterminate. A fully developed sea is one that has reached equilibrium after a steady wind has blown for a sufficiently long time over a sufficiently long fetch. Gravity waves are waves whose celerity (velocity of propagation) is controlled primarily by gravity, as opposed to capillary waves, whose celerity is controlled by the surface tension of the water in which they are traveling. Water waves of length greater than about 51 mm (2 in.) are considered gravity waves. A regular wave is one with a sinusoidal profile as opposed to a trochoidal profile. The wave normal is the local perpendicular to the wave surface, and the wave-normal angle is the angle between the wave normal and the local vertical. The term "encounter" refers to the relative motion between the sea and a ship under way in the sea. Hence the frequency of encounter is the frequency of the sea as viewed from a ship moving through the sea, and not the frequency of the sea relative to an earth-centered, or absolute, coordinate system. Figure B3 shows a typical directional frequency spectrum.

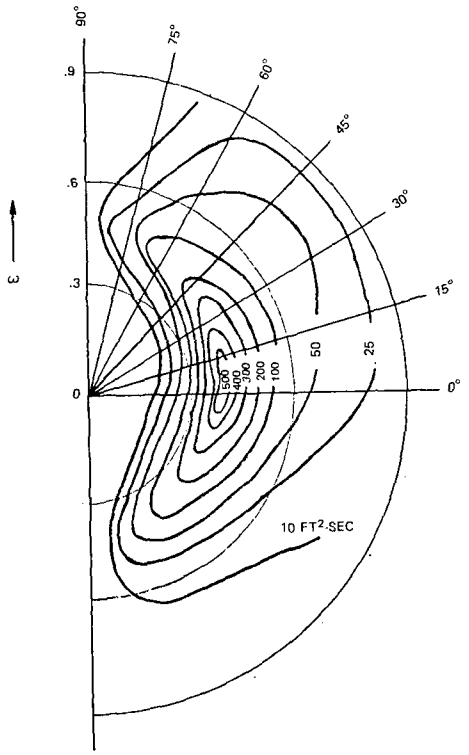

Fig. B3 — Typical directional sea spectrum

☆U.S. GOVERNMENT PRINTING OFFICE:1977 240-824/023 1-3